

Construction of a Cryogenic Microwave Sample Box

Konstruktion eines Tieftemperaturprobenhalters für Mikrowellenversuche

Bachelor Thesis of

Karsten Wolff

At the Department of Physics
Physikalisches Institut (PI)

Reviewer: Prof. Dr. Alexey Ustinov
Advisor: Markus Jerger
Second advisor: Philipp Jung

Duration: 29 May 2012 – 29 October 2012

I hereby declare to have written this work independently and to have listed all used resources and auxiliary material and labeled everything that has been adopted from the work of others.

Ich versichere wahrheitsgemäß, die Arbeit selbstständig angefertigt, alle benutzten Hilfsmittel vollständig und genau angegeben und alles kenntlich gemacht zu haben, was aus Arbeiten anderer unverändert oder mit Abänderungen entnommen wurde.

Zusammenfassung

In dieser Bachelorarbeit wird der Entwurf eines Probenhalters für Quantenbitversuche mit Mikrowellenkopplung bei tiefen Temperaturen beschrieben. Die Probe ist dabei eine runde Leiterplatte mit 5×5 mm großem Chip.

Im Grundaufbau an ein bereits bestehende Design angelehnt, soll der neue Probenhalter im Vergleich weniger Resonanzen von möglichst geringer Qualität aufweisen und dabei kleiner in der Baugröße sein.

Die Montagerichtung ist rechtwinklig zur Achse der zylindrischen Magnetschilde des Kryostaten gewählt. Die Möglichkeit zum direkten Anbringen einer Magnetspule auf dem Sampleholder bleibt bestehen.

Um das Resonanzverhalten der Kavität des Probenhalters zu untersuchen und zu verbessern wurden verschiedene Formen für den Hohlraum simuliert. In dieser Arbeit werden dazu zunächst die physikalischen Grundlagen der elektromagnetischen Wellen über die Maxwell-Gleichungen erarbeitet. In diesem Zusammenhang wird die Wellenausbreitung sowie das Verhalten der Wellen in Hohlräumen beschrieben und die Güte erläutert. Desweiteren wird im Theorieteil ein kurzer Überblick über die mit *CST Microwave Studio* zur Simulation der Resonanzfrequenzen benutzte Jacobi-Davidson-Methode gegeben.

Mit den Simulationen und anschließenden Messungen an realisierten Entwürfen konnte die Tendenz kleinerer Hohlräume zu höheren Resonanzfrequenzen und damit geringerer Transmission bei niedrigeren Frequenzen gezeigt werden. Spezielle Formen der Kavität wie z.B. ungeradzahlige Vielecke, der Torus und andere, sowie deren Kombinationen weisen dabei gute Ergebnisse in bestimmten Frequenzbereichen auf.

Eine Beschichtung des Innenraums mit einem breitbandig absorbierenden Material auf Epoxidharzbasis reduziert stark die Transmission der relevanten Frequenzen. Da hier die Wirkung von der Schichtdicke abhängt, wird empfohlen die Kavität zunächst

größer als benötigt anzufertigen. Nach dem Aufbringen der Beschichtung mit Übermaß erfolgt dann die Nachbearbeitung auf die endgültigen Maße. Damit können deutlich niedrigere Transmissionsraten und eine gute Reproduzierbarkeit erreicht werden. Falls kein Metallgehäuse benötigt wird, kann der gesamte Probenhalter aus dem Absorbermaterial hergestellt werden.

Contents

Zusammenfassung	v
1. Introduction	1
2. Basic Theory	3
2.1. Electrodynamics	3
2.1.1. Maxwell's Equations	3
2.1.2. Propagation of waves	4
2.1.3. Cavities and Quality Factor	5
2.2. Simulation	10
2.2.1. Solver method	10
2.2.2. Settings	13
3. Design of the sample holder	15
3.1. Previously existing design	15
3.2. Demands on a new design	15
3.3. Plugs and cables	16
3.4. New sample holder	16
4. Results	19
4.1. Simulated Eigenmodes	19
4.2. Measured Frequencies	23
5. Conclusion	27
Bibliography	29
Appendix	31
A. Drawings	31
A.1. Cavities	31
A.2. Sample holders	33
B. Simulation Results	35
C. Rosenberger datasheets	43
D. Rogers datasheet	51

E.	Eccosorb datasheet	53
F.	Transmission measurements	55
F.1.	Transmission in the bell shaped cavity	56
F.2.	Transmission in the bell shaped cavity with PCB	59
F.3.	Transmission in the new sample holder	61
F.4.	Transmissionrates compared	62

1. Introduction

The goal of this bachelor thesis is to improve the existing design of a cryogenic microwave sample box for quantum bit experiments. It should be suitable for 5×5 mm chips and fit properly into the cylindrical magnetic shields. The microwave resonances inside the box should be reduced as far as possible since they can be difficult to distinguish from responses of the qubit resonator on the chip. Also it should be possible to manufacture the sample holder with reasonable effort and allow a fast exchange of the samples.

This has been achieved by examining the already existing sample holder and adapting it for the new demands. The cavity has been designed for low resonances with the use of a simulation software, predicting the eigenmodes and allowing comparison of different shapes before mechanically building it. The process of designing the sample box is described in this work as well as the physical principles and the solver method used by the software are explained.

2. Basic Theory

This chapter contains a brief explanation of the basic physical concepts and how to get from Maxwell's equations to standing waves inside a cavity. There will also be a short description of the software used and how the applied solver method works.

2.1. Electrodynamics

2.1.1. Maxwell's Equations

The whole concept of electrodynamics can be described using the four equations by James Clerk Maxwell, which are given in differential, macroscopic form [Fey63],

$$\nabla \cdot \mathbf{E} = \frac{\rho}{\epsilon_0} \quad (2.1)$$

$$\nabla \times \mathbf{E} + \frac{\partial \mathbf{B}}{\partial t} = 0 \quad (2.2)$$

$$\nabla \times \mathbf{B} - \frac{1}{c^2} \frac{\partial \mathbf{E}}{\partial t} = \mu_0 \mathbf{J} \quad (2.3)$$

$$\nabla \cdot \mathbf{B} = 0 \quad (2.4)$$

with \mathbf{E} standing for the electric field, \mathbf{B} for the magnetic field, ρ for the charge density and \mathbf{J} for the current density. In free space, both ρ and \mathbf{J} are zero:

$$\nabla \mathbf{E} = 0 \quad (2.5)$$

$$\nabla \times \mathbf{B} - \frac{1}{c^2} \frac{\partial \mathbf{E}}{\partial t} = 0 \quad (2.6)$$

Taking the curl of equation 2.2 and using the relation $\nabla \times (\nabla \times \mathbf{E}) = \nabla(\nabla \cdot \mathbf{E}) - \nabla^2 \mathbf{E}$ leads together with equation 2.5 to

$$-\nabla^2 \mathbf{E} + \frac{\partial}{\partial t} (\nabla \times \mathbf{B}) = 0.$$

Now applying equation 2.6 gives the wave function for electric waves in free space:

$$\nabla^2 \mathbf{E} - \frac{1}{c^2} \frac{\partial^2 \mathbf{E}}{\partial t^2} = 0. \quad (2.7)$$

A similar approach for equation 2.3 leads to the wave function for magnetic waves in free space:

$$\nabla^2 \mathbf{B} - \frac{1}{c^2} \frac{\partial^2 \mathbf{B}}{\partial t^2} = 0 \quad (2.8)$$

2.1.2. Propagation of waves

By assuming only harmonic time dependence $e^{-i\omega t}$ the equations 2.7 and 2.8 for \mathbf{B} and \mathbf{E} are:

$$\begin{aligned} \nabla^2 \mathbf{E} + \frac{\omega^2}{c^2} \mathbf{E} &= 0 \\ \nabla^2 \mathbf{B} + \frac{\omega^2}{c^2} \mathbf{B} &= 0. \end{aligned}$$

If a plane wave traveling in x-direction, $e^{ikx-i\omega t}$, is considered as solution, it turns out that the wavenumber k and frequency ω are related by the dispersion relation

$$\omega = c \cdot k. \quad (2.9)$$

Therefore, the primordial solution for a plane wave in empty space is

$$\begin{aligned} \psi(x, t) &= ae^{ikx-i\omega t} + be^{-ikx-i\omega t} \\ &= ae^{ik(x-ct)} + be^{-ik(x-ct)}. \end{aligned}$$

In three dimensions, with the convention of only taking the real part of a complex quantity for physical fields and with the wave vector $\vec{k} = k \cdot \vec{n}$, where \vec{n} is a unit vector, the plane wave fields can be written as

$$\begin{aligned}\vec{E}(\vec{x}, t) &= \vec{E}_0 \cdot e^{ik\vec{n}\cdot\vec{x}-i\omega t} \\ \vec{B}(\vec{x}, t) &= \vec{B}_0 \cdot e^{ik\vec{n}\cdot\vec{x}-i\omega t}.\end{aligned}\tag{2.10}$$

With $\nabla \cdot \vec{E} = 0$ and $\nabla \cdot \vec{B} = 0$ in an environment without sources, it is given that $\vec{n} \cdot \vec{E}_0 = \vec{n} \cdot \vec{B}_0 = 0$. This means both, electric and magnetic plane waves are transverse waves.

Until here, all equations have been considered for vacuum. In many materials, the speed of light is different and frequency dependent. Thus, c becomes $c' = \frac{c}{n}$ with the refractive index

$$n = \sqrt{\frac{\mu \cdot \epsilon}{\mu_0 \cdot \epsilon_0}}$$

where $\mu = \mu_r \mu_0$ and $\epsilon = \epsilon_r \epsilon_0$, with the material and frequency dependent constants μ_r and ϵ_r . This equation combines the theory of electromagnetic fields with optics and is sometimes called Maxwell's relation [Nol07]. For more convenient solutions, $\mu \cdot \epsilon$ will be treated as frequency independent. With this, equation 2.9 turns to

$$\omega(k) = \frac{c}{n} \cdot k = v_p \cdot k$$

with the phase velocity v_p . For dispersive media, the group velocity differs from the phase velocity. But since the group velocity is responsible for energy transportation, it can not exceed the speed of light in vacuum. It is given by

$$v_g = \frac{d\omega(k)}{dk}.$$

2.1.3. Cavities and Quality Factor

As a simple cavity, a right circular cylinder with closed top and bottom will be examined. For this geometry it is useful to split the fields in components parallel and transverse to the z axis

$$\begin{aligned}\vec{E} &= \vec{E}_z + \vec{E}_t \\ &= \hat{z}E_z + (\hat{z} \times \vec{E}) \times \hat{z}\end{aligned}$$

with the unit vector \hat{z} . These definitions also apply for the magnetic field \mathbf{B} . By using this the Maxwell equations can be rewritten in transverse and parallel components of the fields [Jac99], where $\nabla_t = (\partial_x, \partial_y, 0)$:

$$\begin{aligned} \frac{\partial \vec{E}_t}{\partial z} + i\omega \hat{z} \times \vec{B}_t &= \nabla_t E_z, & \hat{z} \cdot (\nabla_t \times \vec{E}_t) &= i\omega B_z \\ \frac{\partial \vec{B}_t}{\partial z} + i\mu\epsilon\omega \hat{z} \times \vec{E}_t &= \nabla_t B_z, & \hat{z} \cdot (\nabla_t \times \vec{B}_t) &= i\omega E_z \\ \nabla_t \cdot \vec{E}_t &= -\frac{\partial E_z}{\partial z}, & \nabla_t \cdot \vec{B}_t &= -\frac{\partial B_z}{\partial z}. \end{aligned}$$

By using this, together with the definition for plane waves in equation 2.10 and at least $E_z \neq 0$ or $B_z \neq 0$ in the above Maxwell equations, the results for transverse fields propagating in positive z direction are

$$\begin{aligned} \vec{E}_t &= \frac{i}{\mu\epsilon\omega^2 - k^2} \cdot \left[\frac{\partial}{\partial z} E_z - \omega \hat{z} \times \nabla_t B_z \right] \\ \vec{B}_t &= \frac{i}{\mu\epsilon\omega^2 - k^2} \cdot \left[\frac{\partial}{\partial z} B_z + \mu\epsilon\omega \hat{z} \times \nabla_t E_z \right]. \end{aligned} \quad (2.11)$$

Assuming the cylinder is filled with a lossless dielectric and the walls are made of a perfect electric conductor, the boundary conditions for TM waves are $B_z = 0$ everywhere and $E_z = 0$ at the surface. For TE waves it is $E_z = 0$ everywhere and $\nabla_t B_z = 0$ at the surface.

The fields then behave like a standing wave because of reflections at the top ($z = d$) and bottom $z = 0$ of the cylinder. This only allows waves of the form $A \sin kz + B \cos kz$ which restricts k to $k = p \frac{\pi}{d}$ with $p = 0, 1, 2, \dots$. Together with the boundary conditions, equation 2.11 and $\gamma^2 = \mu\epsilon\omega^2 - k^2$, the equations for TM fields are

$$\begin{aligned} \vec{E}_z &= \psi(x, y) \cos\left(\frac{p\pi z}{d}\right) \\ \vec{E}_t &= \frac{p\pi}{d\gamma^2} \cdot \sin\left(\frac{p\pi z}{d}\right) \nabla_t \psi(x, y) \\ \vec{B}_t &= \frac{i\mu\epsilon\omega}{\gamma^2} \cdot \cos\left(\frac{p\pi z}{d}\right) \hat{z} \times \nabla_t \psi(x, y) \end{aligned}$$

and for TE fields

Table 2.1.: Values for x_{mn} , calculated with *Wolfram Mathematica*

	n=1	n=2	n=3	n=4	n=5
m=0	2.40483	5.52008	8.65373	11.7915	14.9309
m=1	3.83171	7.01559	10.1735	13.3237	16.4706
m=2	5.13562	8.41724	11.6198	14.796	17.9598
m=3	6.38016	9.76102	13.0152	16.2235	19.4094
m=4	7.58834	11.0647	14.3725	17.616	20.8269

$$\begin{aligned}\vec{B}_z &= \psi(x, y) \sin\left(\frac{p\pi t}{d}\right) \\ \vec{E}_t &= -\frac{i\mu\omega}{\gamma^2} \cdot \sin\left(\frac{p\pi z}{d}\right) \hat{z} \times \nabla_t \psi(x, y) \\ \vec{B}_t &= \frac{\mu p \pi}{d \gamma^2} \cdot \cos\left(\frac{p\pi z}{d}\right) \nabla_t \psi(x, y).\end{aligned}$$

Still, γ has to fulfill the two-dimensional wave equation,

$$(\nabla_t^2 + \gamma^2)\psi = 0$$

but now $\gamma^2 = \mu\epsilon\omega - \left(\frac{p\pi}{d}\right)^2$, which for every eigenvalue γ_λ determines an eigenfrequency

$$\omega_{\lambda p}^2 = \frac{1}{\mu\epsilon} \left[\gamma_\lambda^2 + \left(\frac{p\pi}{d}\right)^2 \right].$$

For $p = 0$ and with $\omega = 2\pi f$ the square root of this can be written as

$$f_\lambda = \frac{c' \gamma_\lambda}{2\pi}.$$

For a perpendicular cylinder of radius R and length d with walls of infinite conductivity, the solution of the wave equation for a TM mode $E_z = \psi(\varrho, \Phi)$ with the boundary condition $E_z(R) = 0$ is given by [Jac99]

$$\psi(\varrho, \Phi) = E_0 \cdot J_m(\gamma_{mn}) \cdot e^{\pm im\Phi}$$

Table 2.2.: Values for x'_{mn} , calculated with *Wolfram Mathematica*

	n=1	n=2	n=3	n=4	n=5
m=0	3.83171	7.01559	10.1735	13.3237	16.4706
m=1	1.84118	5.33144	8.53632	11.7060	14.8636
m=2	3.05424	6.70613	9.96947	13.1704	16.3475
m=3	4.20119	8.01524	11.3459	14.5858	17.7887
m=4	5.31755	9.2824	12.6819	15.9641	19.1960

where

$$\gamma_{mn} = \frac{x_{mn}}{R}.$$

x_{mn} is the n th root of the equation $J_m(x) = 0$, where $J_m(x)$ are Bessel functions of the first kind of order m . A few values for x_{mn} are given in table 2.1. The resonance frequencies for TM modes are given by [Jac99]

$$\omega_{mnp} = 2\pi f_{mnp} = \frac{1}{\sqrt{\mu\epsilon}} \sqrt{\frac{x_{mn}^2}{R^2} + \frac{p^2\pi^2}{d^2}} \quad (2.12)$$

This solution still applies for TE modes, but the different boundary condition on $H_z[(\partial\psi/\partial\rho)|_R = 0]$ gives

$$\gamma'_{mn} = \frac{x'_{mn}}{R}$$

where x'_{mn} is the n th root of the derivative of the Bessel functions. A few values for x'_{mn} are given in table 2.2. The resonance frequencies for TE modes are given by [Jac99]

$$\omega_{mnp} = 2\pi f_{mnp} = \frac{1}{\sqrt{\mu\epsilon}} \sqrt{\frac{x'_{mn}{}^2}{R^2} + \frac{p^2\pi^2}{d^2}}$$

With equation 2.12 the first TM eigenmodes for the old sample holder and the smallest possible cavity of the new sample holder have been calculated. The results are shown in table 2.3, where for all modes $p = 0$ except for the 24.7199 GHz mode which has $p = 1$. This clearly shows that a bigger cavity has more resonances at lower frequencies than a smaller one. The results here are almost the same as the ones obtained with *CST Microwave Studio* for copper as cavity walls in tables B.1 and B.2.

The quality factor Q describes the sharpness of response inside a cavity for external excitation. It is defined as 2π times the energy stored inside the cavity, divided by

Table 2.3.: TM eigenmodes in GHz for two cylinders

Mode	Old sample holder R=14.5mm, d=6,4mm	New sample holder R=12mm, d=2.7mm
1	7.91262	9.56108
2	12.6075	15.2341
3	16.8978	20.4182
4	18.1628	21.9467
5	20.9927	25.3662
6	23.0834	27.8925
7	24.7199	33.4652

the energy loss per cycle [Jac99], or in other words the number of cycles it takes for the wave to loose $e^{-2\pi}$ or roughly 0.2% of its energy [Cro98]:

$$Q = \omega_0 \frac{\text{stored energy}}{\text{power loss}} = \omega_0 \frac{U}{P_{loss}}. \quad (2.13)$$

Here, U for each TM mode is given by [Jac99]

$$U = \frac{d\epsilon}{4} \left[1 + \left(\frac{p\pi}{\gamma_\lambda d} \right)^2 \right] \int_A |\psi|^2 da. \quad (2.14)$$

For TM modes with $p = 0$, the result has to be doubled, for TE modes ϵ has to be exchanged for μ . The power loss is given by

$$P_{loss} = \frac{1}{2\sigma\delta} \left[\oint_C dl \int_0^d dz |\vec{n} \times \vec{H}|_{sides}^2 + 2 \int_a da |\vec{n} \times \vec{H}|_{ends}^2 \right] \quad (2.15)$$

where σ is the conductivity of the outer material and $\delta = \sqrt{\frac{2}{\omega\sigma\mu_c}}$ it the skin depth [LTD03] with μ_c being the materials permeability. Inserting equations 2.14 and 2.15 in equation 2.13 and applying further simplifications [Jac99] with ξ_λ being a number of the order unity which depends on the cross section of the cavity, leads to

$$Q = \frac{\mu d}{\mu_c \delta} \frac{1}{2 \left(1 + \xi_\lambda \frac{Cd}{4A} \right)}.$$

Again, for $p = 0$ modes, the result has to be doubled and ξ_λ has to be replaced with $2\xi_\lambda$. C is the circumference and A the cross-sectional cavity of the area. This can be rewritten as

$$Q = \frac{\mu}{\mu_c} \left(\frac{V}{S\delta} \right) \cdot (\text{Geometrical factor})$$

where V is the volume and S the total surface of the cavity. The quality factor for microwave cavities usually is in the order of several hundreds or thousands [Jac99]. For a TE mode in a right circular cylinder with radius R and height d , the geometrical factor is

$$\left(1 + \frac{d}{R}\right) \frac{1 + 0.343 \frac{d^2}{R^2}}{1 + 0.209 \frac{d}{R} + 0.244 \frac{d^3}{R^3}}$$

For the sample holder made from copper, the quality factor is around $Q \approx 10^3 - 10^4$, depending on the shape and size of the cavity, as well as the frequency. The qualities calculated with *CST Microwave Studio* can be found in the tables in appendix B. Coating the cavity with an absorber material like *Eccosorb CR-124* should greatly reduce the Q , since a layer of 1 mm thickness inside the cavity would cause an attenuation of $2 \cdot 1 \cdot 6.7 \text{ dB} = 13.4 \text{ dB}$ or a factor of ≈ 20 according to the datasheet in appendix E. In the presence of resistive losses, where Q has to be a finite value, the resonance frequency is always lowered [Jac99]. For large Q values the resulting resonance frequency is given by

$$\begin{aligned} f_{res} &= \frac{1}{2\pi\sqrt{\mu\epsilon}} \sqrt{\frac{x_{mn}^2}{R^2} + \frac{p^2\pi^2}{d^2}} \cdot \left(1 - \frac{1}{2Q}\right) \\ &= f_0 \cdot \left(1 - \frac{1}{2Q}\right). \end{aligned}$$

2.2. Simulation

The software used in this project was *Autodesk Inventor 2012* for remodeling the designs and creating CAD-models and construction plans. For the simulation of the existing eigenmodes inside the sample holder, *CST Microwave Studio* has been used. All results were obtained by using the built-in eigenmode solver, which was set to use the Jacobi-Davidson method. This method will be explained in the next section.

2.2.1. Solver method

The Jacobi-Davidson method is an iterative approximation method to find the eigenvalues of a symmetric sparse matrix A [HN06]. In this case, the matrix is defined by the wave equations and boundary conditions of the resonant cavity. The basic problem therefore is

$$Au = \lambda u, \quad (2.16)$$

In order to solve this equation, with u and λ being unknown, the first approach is to find an approximation of the exact solution u with [SVdV96]

$$u = u_k + u_k^\perp \quad (2.17)$$

where u_k^\perp is the correction perpendicular to the approximation u_k . The first approximated vector u_k is achieved by applying the Galerkin condition [Hua07] to the problem:

$$v_j^*(Au_k - \lambda_k u_k) = 0 \quad (j, m = 1, 2, \dots, m)$$

where v_1, v_2, \dots, v_m is an orthonormal basis of the subspace $K \perp (Au_k - \lambda_k u_k)$. With $V = [v_1, v_2, \dots, v_m]$ this leads to the problem

$$V^*AVy_k = Hy_k = \lambda_k y_k$$

which has to be solved for the eigenpairs (λ_k, y_k) which provide the approximative solution $u_k = Vy_k$. Per definition, the vectors u_k and u_k^\perp are part of the subspace K for which reason it is interesting to know what happens in K . The projection of A onto K is given by

$$B = (I - u_k u_k^*)A(I - u_k u_k^*)$$

which, with $u_k^*Au_k = \lambda_k$ can be solved for A

$$A = B + Au_k^*u_k + u_k u_k^*A - \lambda_k u_k u_k^*. \quad (2.18)$$

This is used in the basic problem in equation 2.16, which, together with equations 2.17 and 2.18 and respect to $Bu_k = 0$, $u_k^*u_k^\perp = 0$ and $u_k^*u_k = 1$, leads to

$$-r_k = (B - \lambda I)u_k^\perp \quad (2.19)$$

where $r_k = (A - \lambda I)u_k$ is the residual of the approximated original problem. The exact λ is still unknown, so in eq 2.19 it is replaced by λ_k and B is replaced by A [SVdV96]. This leads to

$$-r_k = (I - u_k u_k^*)(A - \lambda_k I)(I - u_k u_k^*)u_k^\perp$$

which with $(I - u_k u_k^*)u_k^\perp = u_k^\perp$ can be written as

$$(A - \lambda_k I)u_k^\perp - \epsilon u_k = -r_k$$

where $\epsilon = u_k^*(A - \lambda_k I)u_k^\perp$. With $M \approx A - \lambda_k I$ the approximation u_k^\perp can be calculated

$$u_k^\perp = \epsilon M^{-1}u_k - M^{-1}r_k$$

Due to u_k and u_k^\perp being defined as perpendicular to each other, multiplying the equation above with u_k^* gives

$$\epsilon = \frac{u_k^* M^{-1} r_k}{u_k^* M^{-1} u_k}$$

In conclusion, the basic idea in pseudocode [Hua07] to find the eigenvalues of the sparse matrix A is

- Choose initial unit vector v_1 , $V_1 \equiv [v_1]$
- Loop for $k = 1, \dots, m$ do:
- Compute $H_k = V_k^* A V_k$ and its eigenpair (λ_k, y_k)
- Compute the vector $u_k \equiv V_k^* y_k$ and the residual r_k
- Stop if convergence is reached
- Else compute the correction u_k^\perp
- $[V_k, u_k^\perp] = V_{k+1}$
- Restart

2.2.2. Settings

Here, for further research and reproducibility of the results, the solver settings used in the CST Microwave Studio are provided. For simulating the cavities, the resonator preset is chosen, setting the dimensions for length to millimeter, for temperature to Kelvin, for frequency to gigahertz and for time to nanoseconds. The background material is set to copper with a conductivity of $5.8 \cdot 10^7$ S/m and a density of 8930 kg/m³. Boundary conditions are left at standard settings. The frequency range was set from 0 GHz to 30 GHz.

The eigenmode solver is set to hexahedral mesh and Jacobi-Davidson-Matrix method. The number of modes is chosen automatically, with adaptive mesh refinement enabled. The desired accuracy in the specials menu is set to 10^{-6} .

3. Design of the sample holder

3.1. Previously existing design

The previously existing sample holder is 37 mm in diameter and 16.5 mm in total height and thus can only be mounted with its axis alligned parallel to the axis of the cylindrical magnetic shields with an inner diameter of 40 mm. This leads to inflexibility about the direction of an applied external magnetic field.

The cavity is able to hold printed circuit boards (PCB) with a diameter of 29 mm, which is bigger than necessary compared to the chip size of 5×5 mm. Also, there is more space left for the plugs than actually needed, which makes the cavity higher and leaves more space for different eigenmodes. The technical drawings of this sample holder can be found in appendix A.15.

3.2. Demands on a new design

The requests on the new design of the sample holder were in general:

- less eigenmodes with a lower quality factor, especially for frequencies below 10 GHz
- smaller size
- easy exchange of the sample
- perpendicular mount to the axis of the magnetic shields
- support for the direct mount of a coil.

To fulfill these requests, the cavity was designed as small as possible, providing just enough space so mount the PCB with its attached chip and sockets for plugs.

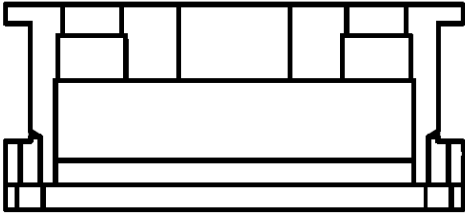


Figure 3.1.: Cross-sectional view of the old sample holder (not to scale)

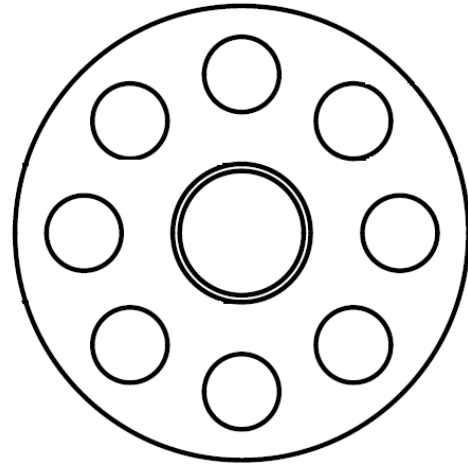


Figure 3.2.: Topview of the old sample holder (not to scale)

3.3. Plugs and cables

The type of plugs was changed from the combination of *Rosenberger Typ 19S602-271L5* and *19K102-K00L5* to *Rosenberger Typ 19K202-271L5*. With these, the cables are directed perpendicular to the plugs, thus allowing a perpendicular mount of the sample holder to the axis of the dipstick. Also the minimum height of the sample holder is significant smaller than before. By putting the cylindrical part of the plugs on the PCB *Rosenberger Typ 19S102-40ML5* inside a slightly larger bore in the sample holder, the height can be reduced even more. Datasheets are attached in appendix C.

The change from semi-rigid to flexible cables provides the possibility to bend them in any desired direction. This is also necessary for a mount perpendicular to the dipstick.

Regarding the size of the chip and plugs, the size of the cavity was set do be 24mm in diameter and 2mm of free space above the PCB. Different designs have been tested, in order to reduce and/or shift the eigenmodes to another frequency range.

3.4. New sample holder

The new sample holder adapts the same basic outer shape as the old one, using the same method for mounting the insertion of the PCB and a similar recess for the coil. A design with a screwless mount of the PCB has been discussed, but has been discarded due to its inevitably larger size. The rims holding the coil in place are just as thick as necessary to hold the threads for mounting the bottompart and still

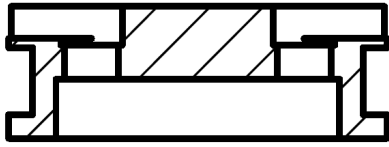


Figure 3.3.: Cross-sectional view of the new sample holder (not to scale)

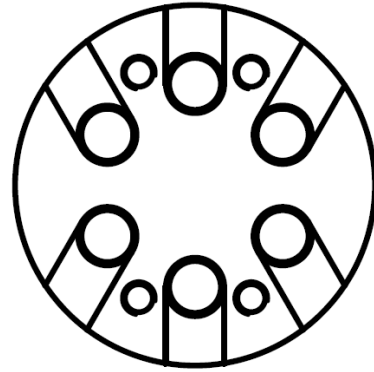


Figure 3.4.: Top view of the new sample holder (not to scale)

grant enough mechanical stability to keep the coil safe from damage. This leaves a maximum of space for the coil.

On the topside of the sample holder, there are up to six sockets for plugs, arranged rotation symmetric. The cutouts for the cables are wide enough to fit in also the soldering points connecting the plugs to the cables. There is no need for a lid to keep the plugs in place because the top of the sample holder and the plugs fit even and the sample holder is directly screwed with its top to the mounting plate inside the cryostat. To provide room for the threads for these screws, the cutouts for the cables are arranged radiant.

Due to the perpendicular cable mount in the plugs, this sample holder is referred to as *sample holder, Right Angle Jack*, or *SH RAJ*. A schematic view of this sample holder can be found in figures 3.3 and 3.4. For the full drawings see appendix A.17.

4. Results

4.1. Simulated Eigenmodes

In this section the simulated eigenmodes of different cavity designs will be discussed. The basic idea in general cavity design is to modify the angle of the walls in a way that parallel surfaces are avoided. This is meant to reduce the possibilities for standing waves. Altogether, six types of designs in different variations have been simulated:

- The smallest possible cavity, a simple cylindrical shape with just enough room for the plugs. Fig. 4.1.
- A dome above the basic shape. Fig. 4.2.
- A cone atop the basic cylinder. Fig. 4.3.
- A bell shaped cavity. The bell is designed by setting a smaller cylinder atop the base cylinder. Then the edges are rounded. Fig. 4.4.
- A torus. With this shape, the plugs on the PCB fit completely inside the cavity and only bores for the smaller plugs attached to the cables are necessary. Fig. 4.5.
- A septagon instead of the basic cylinder, inscribed into the same diameter. Here, there are no parallel surfaces on the side. Compared to a pentagon this shape provides more space for the plugs without the need for a bigger sample holder. This has been combined with a bell shape. Fig. 4.6.

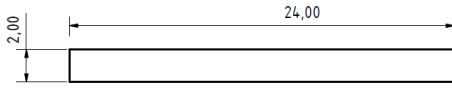


Figure 4.1.: Smallest cylindrical cavity

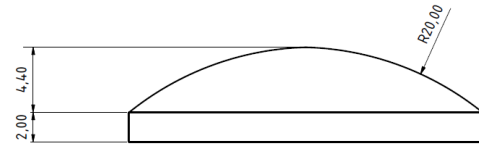


Figure 4.2.: Dome shaped cavity

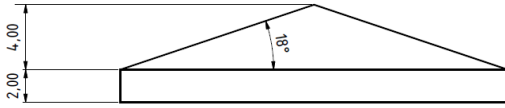


Figure 4.3.: Cone shaped cavity

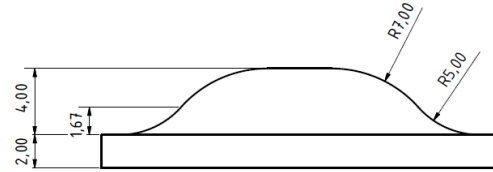


Figure 4.4.: Bell shaped cavity

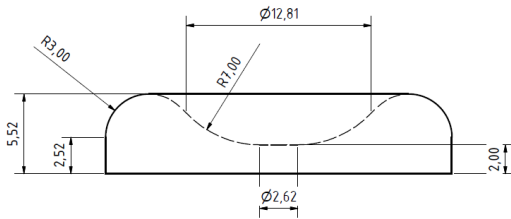


Figure 4.5.: Torus

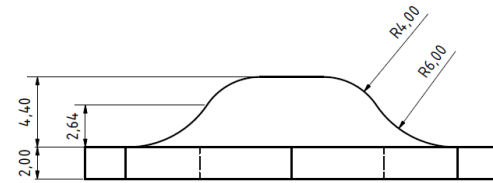


Figure 4.6.: Septagon

The drawings for the different varieties of the cavity can be found in appendix A.1. The eigenmodes have been simulated in the frequency range from 0 - 30 GHz. In this section, the first ten eigenmodes for each shape are listed, assuming a perfect electric conductor as background material. For the full result tables as given by CST MWS, see appendix B. The full tables also contain the computed quality factors, assuming copper as surrounding material.

To distinguish the different bell shapes in the table, the dimensions are given as a name. For example *Bell d10 h4 r7 r5* stands for a bell whose underlying cylinder is 10 mm in diameter and 4 mm in height. The upper edge is rounded with a radius of 7 mm, the edge connecting the base cavity with the bell is rounded with a radius of 5 mm. The addition *DE* means a layer of dielectric has been added underneath the cavity.

According to the results in table 4.1, the combination of a septagonal base shape with a bell shaped cavity on top produces the highest frequency for the first eigenmode. Since this design is not rotation symmetrical and therefore difficult to manufacture, the bell version with the highest frequency as first eigenmode was preferred, in order to keep the eigenmodes out of the frequency range between 8GHz and 12GHz [JPM⁺11]. In this context, the torus cavity would also be interesting, but has not been build yet.

The simulations with an additional, 0.7 mm thick layer of the dielectric *Rogers TMM 10i (loss free)*, datasheet in appendix D, show a drop in the frequencies. This material has a dielectric constant of $\epsilon_r = 9.8$ and the same thermal expansion as copper. The results of these simulations are only to be treated as an approximation to the real PBCs, which consists of 0.63 mm dielectric, covered on both sides with 35 μm of copper. Adding this layer to the simulation would have taken too much time to compute. Also adding the plugs to the simulation took an unreasonably long time to compute and therefore they were left out. The plugs are mandatory inside the sample holder, independent of which cavity design is chosen, so their presence in the simulation does not change the selection of the cavity.

Table 4.1.: The first 10 eigenmodes, as given by CST MWS. Frequencies in GHz.

Cavity	Fig.	Tab.	1	2	3	4	5
Cylinder org	A.1	B.1	7,9123	12,6051	12,6051	16,8890	16,8936
Cylinder small	A.2	B.2	9,5589	15,2249	15,2249	20,3891	20,4031
Dome	A.3	B.3	11,0323	16,2804	16,2804	21,2063	21,2204
Torus	A.4	B.4	7,4734	15,2047	15,2048	21,1081	21,1205
Torus DE		B.5	7,0619	13,7140	13,7141	18,7331	18,7354
Cone big	A.5	B.6	11,0660	16,0270	16,0271	20,9701	20,9814
Cone small	A.6	B.7	11,5428	15,8653	15,8654	20,4661	20,4783
Bell d8 h4 r4 r4	A.7	B.8	10,5803	14,6992	14,6993	19,8596	19,8671
Bell d10 h4,4 r7 r7	A.8	B.9	11,7161	16,1245	16,1247	20,6802	20,6806
Bell d10 h4 r7 r5	A.10	B.10	11,5916	15,6904	15,6905	20,1953	20,2042
Bell d12 h3 r4 r6 DE		B.11	9,7701	13,4486	13,4487	17,3120	17,3145
Bell d12 h4 r4 r6	A.11	B.12	11,5501	15,5852	15,5854	20,1540	20,1627
Bell d12 h4 r6 r6	A.12	B.13	11,2975	15,2800	15,2802	19,9795	19,9887
Bell d14 h4 r6 r15	A.13	B.14	11,3504	15,8137	15,8154	20,6009	20,6153
Septagon Bell	A.14	B.15	12,3882	16,8174	16,8185	21,7730	21,7777

Cavity	Fig.	Tab.	6	7	8	9	10
Cylinder org	A.1	B.1	18,1541	20,9798	20,9798	23,0654	23,0654
Cylinder small	A.2	B.2	21,9178	25,3243	25,3243	27,8347	27,8347
Dome	A.3	B.3	22,4162	25,9648	25,9649	27,8205	27,8205
Torus	A.4	B.4	22,0251	26,3604	26,3604	27,5379	27,5380
Torus DE		B.5	19,3426	22,7000	22,7000	23,4727	23,4728
Cone big	A.5	B.6	22,5548	25,7809	25,7810	28,0317	28,0318
Cone small	A.6	B.7	21,9516	25,1141	25,1141	27,4138	27,4139
Bell d8 h4 r4 r4	A.7	B.8	23,1041	24,9700	24,9700	27,9938	27,9940
Bell d10 h4,4 r7 r7	A.8	B.9	21,7481	25,3223	25,3223	27,3636	27,3636
Bell d10 h4 r7 r5	A.10	B.10	21,5995	24,8695	24,8696	27,5209	27,5210
Bell d12 h3 r4 r6 DE		B.11	19,1307	20,9300	20,9300	23,4659	23,4659
Bell d12 h4 r4 r6	A.11	B.12	21,7442	24,8861	24,8861	27,5698	27,5699
Bell d12 h4 r6 r6	A.12	B.13	22,1138	24,8078	24,8078	27,7245	27,7246
Bell d14 h4 r6 r15	A.13	B.14	22,3702	25,3613	25,3641	27,7421	27,7454
Septagon Bell	A.14	B.15	23,5455	26,7357	26,7393	29,2878	29,2880

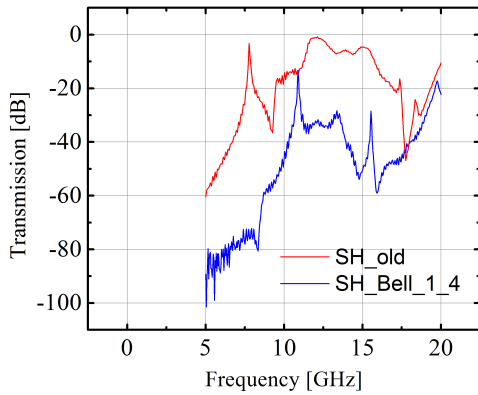


Figure 4.7.: Transmission in the old and bell shaped cavity

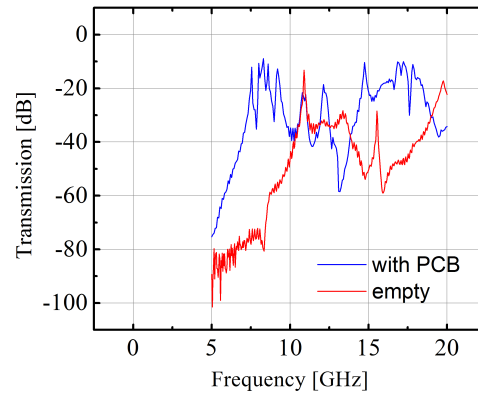


Figure 4.8.: Bell cavity with and without PCB

4.2. Measured Frequencies

Out of the possible cavities, the bell as in fig. A.7 and the basic small cylinder have been built. The bell shaped cavity has been set into a sample holder akin to the old design, but with smaller dimensions overall. Drawings are attached in appendix A.16.

The transmission of microwave frequencies has been measured with a network analyzer. For the old sample holder and the bellshaped cavity this has been done without a PCB inside, by removing the lashes on one side of the *19K102-K00L5* adaptor to create a small antenna. To actually measure a transmission, one emitting and one receiving antenna was used. The measured transmission through the cables directly connected to each other and bigger pictures of the other measurements are in appendix **Transmission measurements**.

The measurements with a PCB included in the bellshaped cavity and the new sample holder were done with two plugs of type *19S102-40ML5* facing each other with the small appendage acting as antenna.

The peaks of the transmission measurements for the big, original cylinder and the bell cavity [Fig. 4.7] are in sufficient accordance with the simulated eigenmodes, which shows that the simulation gives a good survey of which cavity to choose. With the bell shaped cavity, the transmission between 9 and 10 GHz drops about 35 dB. Different positions of the plugs to each other as well as closing the empty sockets with aluminium tape did not affect the lower eigenfrequencies in a significant way. For the different positions and measurements with and without tape, see appendix **Transmission in the bell shaped cavity**.

Adding the PCB to the bell shaped cavity [Fig.4.8] gives a higher transmission, specially around and below 9 GHz. The basic pattern of peaks is shifted to lower frequencies. A reason for the numerous additional peaks could be the plugs inside the cavity or the PCB with $\epsilon_r = 9.8$, creating further resonances and surface effects.

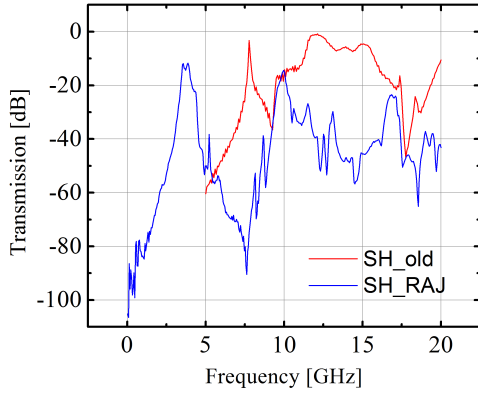


Figure 4.9.: Transmission in the big (without PCB) and small cylinder (with PCB)

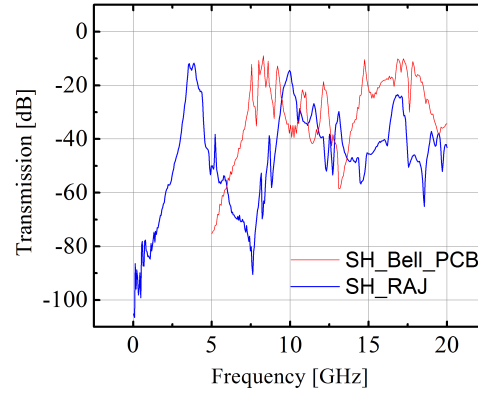


Figure 4.10.: Comparison of bell and small cylinder, with PCB

The new sample holders basic cylindrical cavity has only been measured with the PCB mounted, due to the other plugs used. This is also the reason the transmission has a peak at 10 GHz, as high as the transmission in the bigger cylinder [Fig. 4.9]. Comparing the bell shaped cavity with the small basic cylinder shows that the transmission inside the bell is up to 25 dB lower at 10 GHz than in the cylinder [Fig. 4.10].

In the next step, both of the smaller cavities have been coated with *Eccosorb CR-124*, a microwave absorbing epoxy based resin. The absorbing abilities result of ferromagnetic particles diluted in the resin. The full datasheet can be found in appendix E.

In the cylinder, only the top has been covered approximately 0.5 mm thick with Eccosorb, while inside the bell every wall but the bottom where the PCB sits has been covered. This has been done by first applying the Eccosorb and then removing everything that blocked the correct fit of the PBC and plugs with a power tool. According to the different application of the Eccosorb, the damping results differ for both cavities.

While inside the bell the transmission has decreased by about 30 dB for frequencies below 10 GHz, it has been reduced by about 60 dB for frequencies over 15 GHz [Fig. 4.12]. The cylinder shows a drop of 20 dB around 10 GHz [Fig. 4.11].

With the Eccosorb applied, both cavity designs show an overall reduction of the transmission, especially for frequencies over 10 GHz. Comparing the transmission rates of the coated with the uncoated cavities makes obvious that the reduction of transmission strongly depends on the amount of Eccosorb inside the cavity.

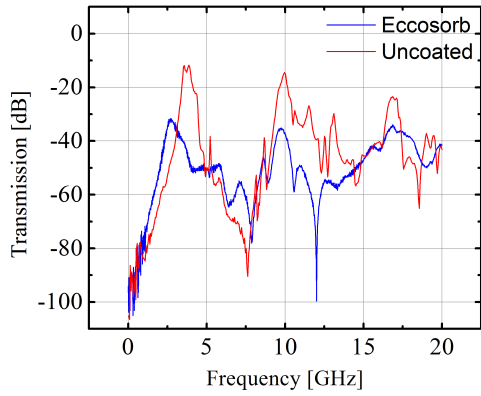


Figure 4.11.: SH RAJ with and without Eccosorb, with PCB

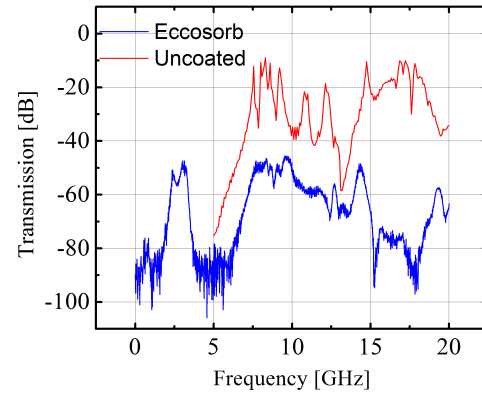


Figure 4.12.: Bell with and without Eccosorb, with PCB

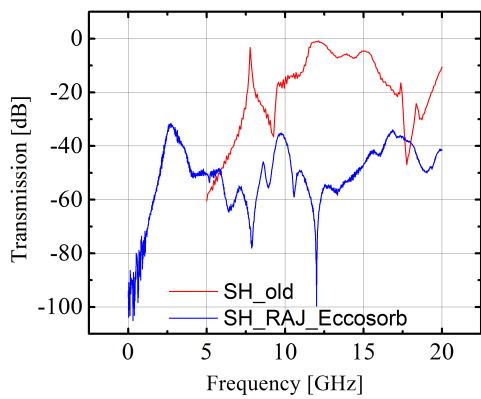


Figure 4.13.: Small cylinder with PCB and Eccosorb compared to the old cavity

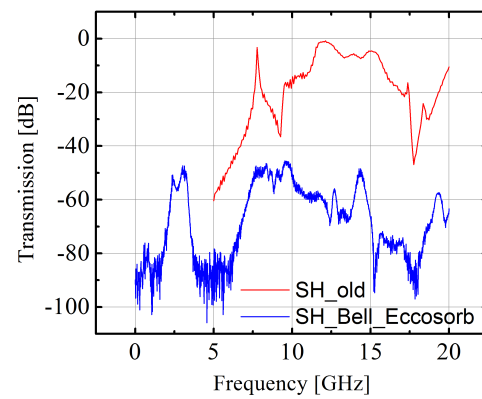


Figure 4.14.: Bell cavity with PCB and Eccosorb compared to the old cavity

5. Conclusion

In general the new design of the sampleholder serves the requirements for a mount to perpendicular to the axis of the magnetic shields, while being small enough to bear a magnetic coil without additional support. The previous orientation of mounting can still be realized with a small adapter. The tendency of smaller cavities to have higher resonance frequencies and thus reduced transmission at lower frequencies could be shown.

The sharp drops of the transmission at some frequencies indicate the potential in designing cavities with low transmission rates for specific frequency ranges. Further simulations with a more powerful computer could increase the accuracy of the simulations, with correct models of the PCB and plugs included. Different shapes, for example the torus, odd numbered n-edged basic cavities or even combinations of both could show excellent results for specific frequency ranges.

Coating the inside of the cavity with a broadband absorber like Eccosorb drastically reduces the transmission for most frequencies, though it depends on the thickness and where it is applied. Milling out the cavity bigger than needed and then filling it up with Eccosorb before finishing the sampleholder can provide a much thicker and smoother coating and thus much lower transmission rates and better reproducibility. If a full metal casing is not necessary, the full sampleholder can be made out of Eccosorb.

Bibliography

- [Cro98] B. Crowell, *Light and Matter - Open Source Physics Textbooks*, August 3, 2007 1998, vol. 2012, no. 24 October 2012. [Online]. Available: <http://www.lightandmatter.com>
- [Fey63] R. Feynman, *The Feynman Lectures on Physics: Volume 2*. Boston: Addison-Wesley, 1963, vol. 2.
- [HN06] M. E. Hochstenbach and Y. Notay, “The Jacobi–Davidson method,” *GAMM-Mitt.*, vol. 29, no. 2, pp. 368–382, 2006.
- [Hua07] C.-a. Huang, “An introduction to jacobi-davidson method,” 2007. [Online]. Available: http://www.math.nuk.edu.tw/jinnliu/software_Engineering/JD_PDF.pdf
- [Jac99] J. D. Jackson, *Classical electrodynamics*, 3rd ed. New York: Wiley, 1999. [Online]. Available: <http://swbplus.bsz-bw.de/bsz072816562cov.htm>
- [JPM⁺11] M. Jerger, S. Poletto, P. Macha, U. Huebner, A. Lukashenko, E. Il’ichev, and A. V. Ustinov, “Spectroscopy of a qubit array via a single transmission line,” 2011.
- [LTD03] D. Lioubtchenko, S. Tretyakov, and S. Dudorov, *Millimeter wave waveguides*. Boston, Mass. [u.a.]: Kluwer Academic, 2003, : £74.00. [Online]. Available: <http://swbplus.bsz-bw.de/bsz112981828cov.htm>
- [Nol07] W. Nolting, Ed., *Grundkurs Theoretische Physik*, 8th ed. Berlin: Springer, 2007, vol. 3: Elektrodynamik. [Online]. Available: <http://swbplus.bsz-bw.de/bsz263309940cov.htm>
- [SVdV96] G. L. G. Sleijpen and H. A. Van der Vorst, “A jacobi–davidson iteration method for linear eigenvalueproblems,” *SIAM J. Matrix Anal. Appl.*, vol. 17, no. 2, pp. 401–425, Apr. 1996. [Online]. Available: <http://dx.doi.org/10.1137/S0895479894270427>

Appendix

A. Drawings

A.1. Cavities

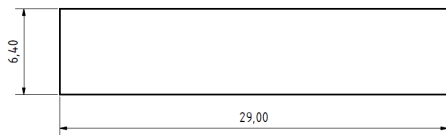


Figure A.1.: d29 h64

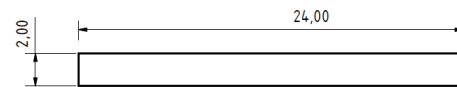


Figure A.2.: d24 h2

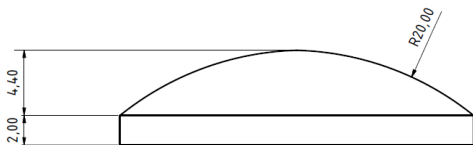


Figure A.3.: Dome h4.4 r20

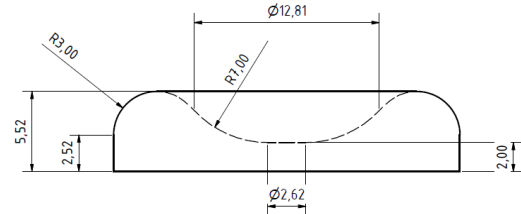


Figure A.4.: Torus

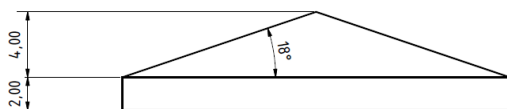


Figure A.5.: Big Cone

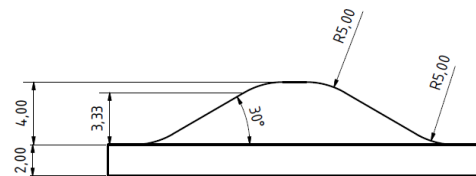


Figure A.6.: Small cone

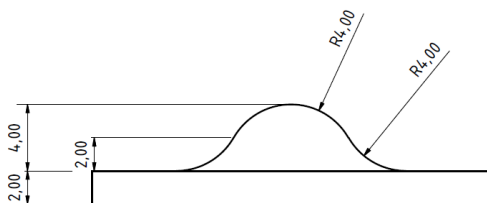


Figure A.7.: Bell h4 d8 r4 r4

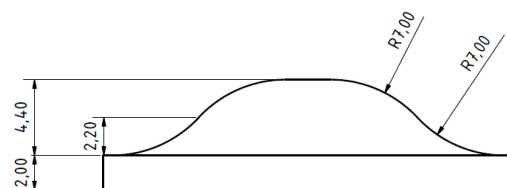


Figure A.8.: Bell h4.4 d10 r7 r7

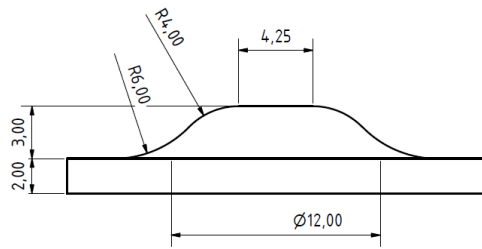


Figure A.9.: Bell h3 d12 r4 r6

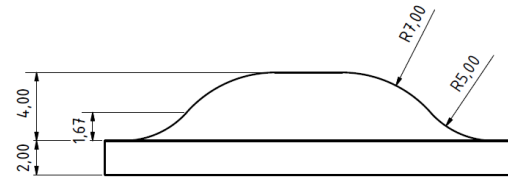


Figure A.10.: Bell h4 d10 r7 r5

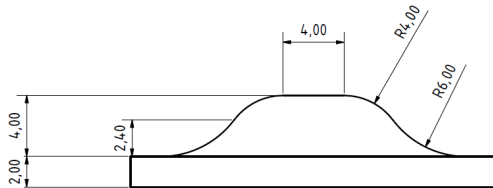


Figure A.11.: Bell h4 d12 r4 r6

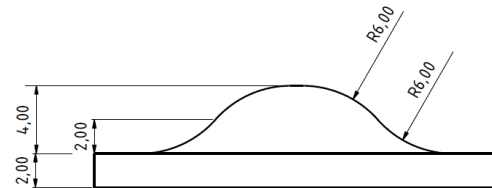


Figure A.12.: Bell h4 d12 r6 r6

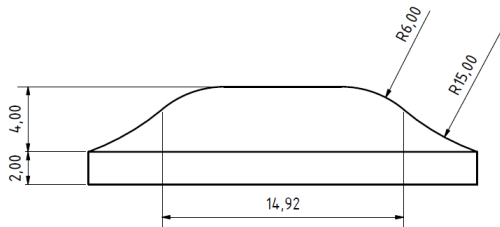


Figure A.13.: Bell h4 d14 r6 r15

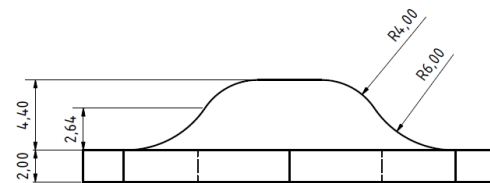


Figure A.14.: Septagon bell h4 d12 r6 r6

A.2. Sample holders

Figure A.15.: Drawing of the old sample holder

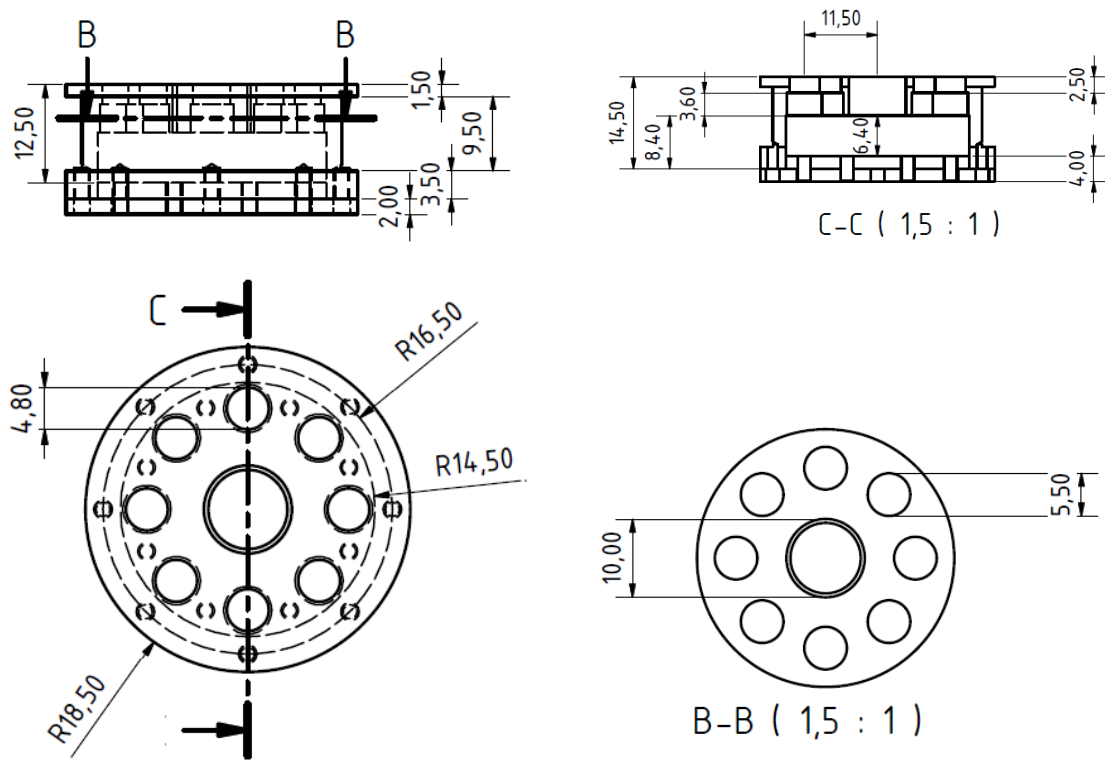


Figure A.16.: Drawing of the bell cavity sample holder

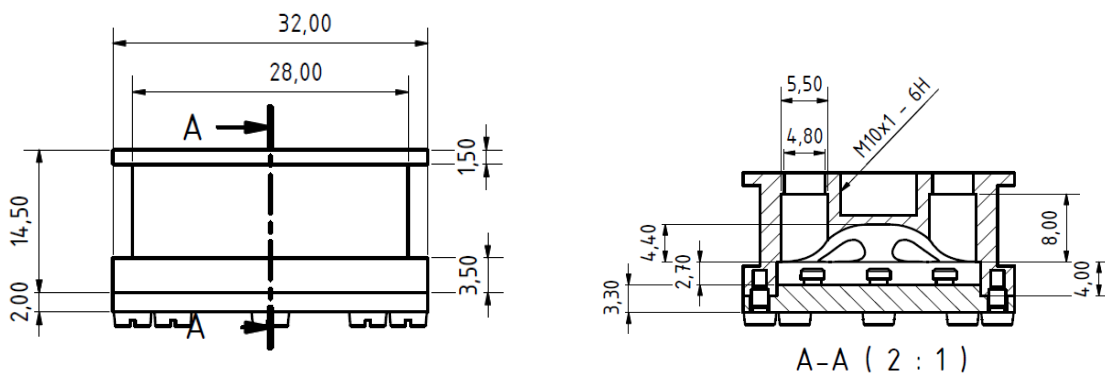
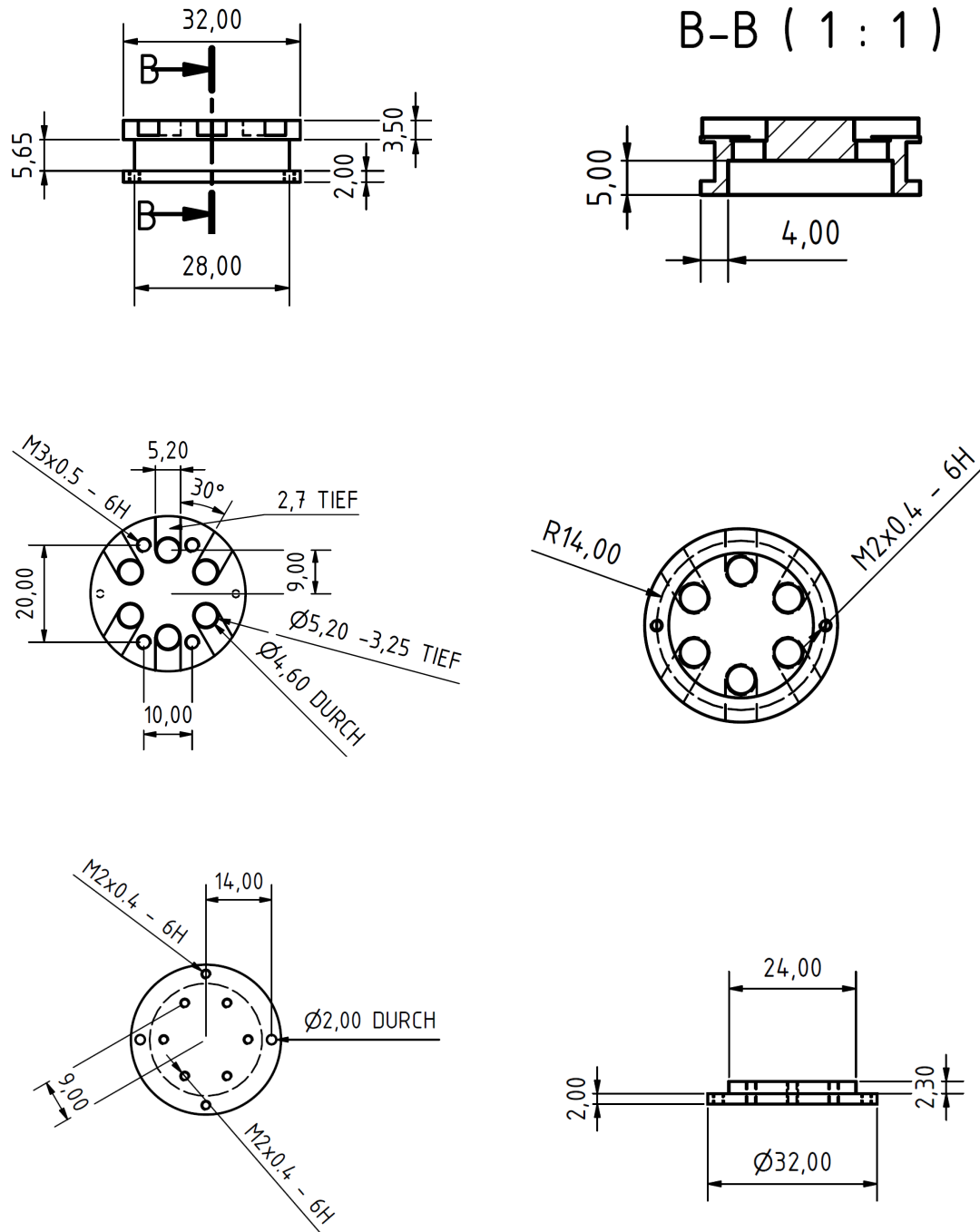


Figure A.17.: Drawing of the RAJ sample holder



B. Simulation Results

Table B.1.: Cavity Org d28 h6.4

Mode	Frequency [Ghz]	$ (\mathbf{Ax}-\mathbf{x})/\mathbf{x} $	max(e)	div(e)	Q-Factor
1	7.91229006307	3.79e-007	1.89e-006	4.49e-016	5.9991e+003
2	12.6051288071	3.69e-008	9.93e-008	1.68e-016	7.5817e+003
3	12.6051288071	1.30e-008	4.79e-008	4.71e-016	7.5818e+003
4	16.8890270974	3.68e-007	1.26e-006	2.80e-016	8.7748e+003
5	16.8935946339	2.47e-007	9.82e-007	3.96e-016	8.8075e+003
6	18.1540875462	4.17e-008	1.16e-007	3.75e-016	9.1205e+003
7	20.979842112	5.68e-007	2.32e-006	3.05e-016	9.8169e+003
8	20.979842112	9.96e-007	5.08e-006	1.76e-016	9.8162e+003
9	23.0654363263	3.64e-007	7.51e-007	3.72e-016	1.0308e+004
10	23.0654363263	7.06e-007	2.11e-006	1.70e-016	1.0308e+004
11	24.1364356492	7.49e-008	2.38e-007	2.96e-016	7.7153e+003
12	24.1364356492	9.89e-007	3.15e-006	2.98e-016	7.7151e+003
13	24.6665908956	9.62e-007	5.46e-006	1.74e-016	6.6474e+003
14	24.9455202653	2.00e-007	6.20e-007	1.78e-016	1.0724e+004
15	24.9466470832	5.40e-007	1.53e-006	3.37e-016	1.0733e+004
16	25.4323345035	2.96e-007	8.14e-007	4.16e-016	7.8656e+003
17	25.4327619501	8.75e-007	5.70e-006	4.34e-016	7.8883e+003
18	26.5466696459	6.64e-007	1.96e-006	4.41e-016	6.9043e+003
19	26.5466696459	8.38e-008	2.18e-007	4.49e-016	6.9043e+003
20	26.5476969194	4.87e-007	2.09e-006	3.17e-016	1.0261e+004
21	27.1442785565	2.17e-007	8.31e-007	4.09e-016	8.2294e+003
22	27.1442785565	3.41e-007	1.56e-006	3.00e-016	8.2296e+003
23	27.6553412104	3.22e-007	1.65e-006	1.74e-016	1.1341e+004
24	27.6722123054	1.00e-006	2.81e-006	3.30e-016	1.1305e+004
25	28.4384438525	4.82e-007	1.86e-006	4.06e-016	1.1488e+004
26	28.8269149566	7.55e-007	2.66e-006	1.77e-016	1.1564e+004
27	28.8269149566	7.15e-007	3.99e-006	3.94e-016	1.1561e+004
28	28.8279124186	9.31e-007	7.06e-006	4.47e-016	7.1964e+003
29	28.8315315363	9.54e-007	5.11e-006	1.89e-016	7.2145e+003
30	29.1824016422	2.95e-007	1.29e-006	1.84e-016	8.7128e+003
31	29.1844053387	2.00e-007	9.94e-007	1.86e-016	8.6134e+003
32	29.2120724764	6.44e-007	1.91e-006	3.10e-016	1.2167e+004
33	29.2120724764	9.08e-007	2.42e-006	4.16e-016	1.2167e+004
34	29.5872867029	4.24e-007	2.62e-006	3.18e-016	7.3038e+003

Table B.2.: cavity d24 h2

Mode	Frequency [Ghz]	$ (\mathbf{Ax}-\mathbf{x})/\mathbf{x} $	$\max(\mathbf{e})$	$\text{div}(\mathbf{e})$	Q-Factor
1	9.55886900743	8.57e-014	3.14e-013	4.10e-016	2.5463e+003
2	15.2249433371	9.98e-012	1.41e-010	3.37e-016	3.2261e+003
3	15.2249433371	1.63e-013	1.15e-012	3.22e-016	3.2231e+003
4	20.3891230931	8.02e-007	1.13e-005	2.30e-016	3.7439e+003
5	20.4030622364	7.17e-007	8.76e-006	2.57e-016	3.7522e+003
6	21.9178398831	1.37e-008	1.34e-007	3.07e-016	3.8938e+003
7	25.3243254524	5.35e-008	1.09e-007	2.53e-016	4.1936e+003
8	25.3243254524	3.95e-008	1.09e-007	2.94e-016	4.1969e+003
9	27.8346845507	3.91e-008	1.58e-007	3.56e-016	4.4179e+003
10	27.8346845507	4.03e-007	4.47e-006	3.02e-016	4.4118e+003

Table B.3.: Dom

Mode	Frequency [Ghz]	$ (\mathbf{Ax}-\mathbf{x})/\mathbf{x} $	$\max(\mathbf{e})$	$\text{div}(\mathbf{e})$	Q-Factor
1	11.0322747325	3.60e-007	7.69e-006	3.73e-016	5.1652e+003
2	16.2804151586	1.97e-011	2.33e-010	4.19e-016	6.0423e+003
3	16.2804274558	6.97e-009	1.29e-007	1.94e-016	6.0196e+003
4	21.2063472814	9.76e-008	1.82e-006	4.33e-016	6.5978e+003
5	21.2204077118	1.55e-007	2.96e-006	4.80e-016	6.4063e+003
6	22.4162009475	9.70e-009	1.74e-007	1.98e-016	6.9688e+003
7	25.9648171474	2.57e-007	3.65e-006	3.12e-016	6.5841e+003
8	25.9648581763	4.96e-008	8.33e-007	4.23e-016	6.6027e+003
9	27.8204555347	2.58e-007	3.71e-006	1.80e-016	7.4314e+003
10	27.8204730491	4.62e-007	2.26e-006	3.39e-016	7.4984e+003
11	28.2100987931	2.85e-007	4.08e-006	4.40e-016	7.7593e+003
12	28.2100995578	2.79e-007	3.03e-006	1.99e-016	7.7693e+003

Table B.4.: torus

Mode	Frequency [Ghz]	$ (\mathbf{Ax}-\mathbf{x})/\mathbf{x} $	$\max(\mathbf{e})$	$\text{div}(\mathbf{e})$	Q-Factor
1	7.47340218665	2.09e-009	7.07e-009	2.74e-016	4.2816e+003
2	15.2047282967	1.56e-007	9.00e-007	4.36e-016	4.9860e+003
3	15.2047653528	3.44e-008	1.12e-007	1.80e-016	4.8946e+003
4	21.1081426525	2.60e-008	8.63e-008	2.02e-016	6.3874e+003
5	21.120470321	6.80e-008	1.90e-007	4.36e-016	5.7334e+003
6	22.025117825	4.27e-007	1.59e-006	1.94e-016	5.5202e+003
7	26.3604242429	9.67e-007	4.06e-006	4.58e-016	6.9157e+003
8	26.3604281791	6.20e-008	1.34e-007	3.39e-016	6.9137e+003
9	27.5379142348	9.35e-007	2.80e-006	1.89e-016	6.1027e+003
10	27.5380044037	8.60e-007	6.43e-006	3.48e-016	6.1069e+003
11	29.7130093694	3.57e-007	1.49e-006	3.00e-016	4.8169e+003

Table B.5.: Torus DE

Mode	Frequency [Ghz]	$ (\mathbf{Ax}-\mathbf{x})/\mathbf{x} $	$\max(\mathbf{e})$	$\text{div}(\mathbf{e})$	Q-Factor
1	7.0618587786	1.08e-005	5.28e-005	4.80e-015	4.6408e+003
2	13.7140431111	1.94e-005	5.60e-005	1.41e-014	4.9886e+003
3	13.7140677291	1.73e-006	3.01e-006	1.10e-014	4.9892e+003
4	18.7330962267	3.54e-005	2.76e-004	1.15e-015	5.0239e+003
5	18.7353955849	7.88e-005	2.45e-004	3.32e-015	4.9868e+003
6	19.3426032302	4.75e-005	7.50e-005	2.21e-015	4.5867e+003
7	22.7000276576	4.46e-005	8.26e-005	1.30e-014	4.2240e+003
8	22.700029392	8.52e-005	3.40e-004	1.52e-014	4.2246e+003
9	23.4727195591	9.25e-005	1.15e-004	3.08e-014	3.7100e+003
10	23.4727558102	6.67e-005	8.65e-005	2.78e-014	3.7111e+003
11	24.7950845105	6.11e-005	2.12e-004	1.89e-014	3.3150e+003

Table B.6.: Kegel d24 h2 h4

Mode	Frequency [Ghz]	$ (\mathbf{Ax-x})/\mathbf{x} $	$\max(\mathbf{e})$	$\text{div}(\mathbf{e})$	Q-Factor
1	11.0659511406	6.72e-008	3.89e-007	3.90e-016	4.1150e+003
2	16.0270203919	5.58e-007	2.36e-006	4.36e-016	4.9160e+003
3	16.0270919026	2.75e-007	1.08e-006	2.82e-016	4.9044e+003
4	20.9700728439	4.56e-007	2.33e-006	4.16e-016	5.4757e+003
5	20.9813501687	4.79e-007	2.12e-006	3.35e-016	5.5070e+003
6	22.5548137763	9.10e-007	6.33e-006	4.47e-016	6.2907e+003
7	25.7809293837	1.61e-007	5.92e-007	1.94e-016	5.9594e+003
8	25.7809592846	2.16e-007	1.74e-006	4.76e-016	5.9503e+003
9	28.0316997693	2.54e-007	1.25e-006	1.91e-016	6.9122e+003
10	28.0318320838	9.10e-007	4.76e-006	3.23e-016	6.9177e+003

Table B.7.: Kegel d18 h4 a60 r5 5

Mode	Frequency [Ghz]	$ (\mathbf{Ax-x})/\mathbf{x} $	$\max(\mathbf{e})$	$\text{div}(\mathbf{e})$	Q-Factor
1	11.5428080033	1.44e-013	1.32e-012	3.71e-016	3.3270e+003
2	15.8652674549	1.16e-008	1.01e-007	4.66e-016	3.7744e+003
3	15.8653739455	9.83e-009	9.61e-008	4.76e-016	3.7676e+003
4	20.4661335901	7.38e-007	9.85e-006	4.24e-016	4.1252e+003
5	20.4782845391	3.83e-009	5.50e-008	4.42e-016	4.1396e+003
6	21.9515576588	1.39e-008	1.38e-007	2.65e-016	5.3118e+003
7	25.1140821873	1.42e-008	1.38e-007	3.40e-016	4.4914e+003
8	25.114125511	1.66e-008	1.00e-007	3.80e-016	4.4940e+003
9	27.4137896997	7.40e-008	8.66e-007	4.02e-016	5.9148e+003
10	27.4139137888	2.06e-008	7.44e-008	2.07e-016	5.9192e+003
11	29.7415023695	5.93e-008	6.68e-007	4.31e-016	4.9717e+003
12	29.7431755933	3.17e-007	3.41e-006	1.92e-016	4.2861e+003

Table B.8.: Glocke d8 h4 r4 r4

Mode	Frequency [Ghz]	$ (\mathbf{Ax}-\mathbf{x})/\mathbf{x} $	$\max(\mathbf{e})$	$\text{div}(\mathbf{e})$	Q-Factor
1	10.5803026296	6.06e-009	6.85e-008	3.47e-016	2.6712e+003
2	14.6991920667	2.11e-007	8.14e-007	4.48e-016	3.3719e+003
3	14.699349158	4.23e-007	1.39e-006	2.66e-016	3.3751e+003
4	19.8596337747	1.52e-007	8.65e-007	3.52e-016	3.8981e+003
5	19.8670781487	4.33e-007	1.71e-006	3.46e-016	3.8430e+003
6	23.1041243536	5.63e-007	1.62e-006	4.56e-016	4.9432e+003
7	24.9699918747	1.96e-007	1.11e-006	1.95e-016	4.2500e+003
8	24.9700007197	6.16e-007	2.08e-006	3.31e-016	4.2503e+003
9	27.993797994	7.40e-008	5.51e-007	4.57e-016	4.9514e+003
10	27.9939631857	7.91e-007	4.08e-006	3.15e-016	4.9525e+003
11	29.9033525446	7.71e-007	5.19e-006	3.19e-016	4.5858e+003
12	29.9047205208	8.50e-008	4.26e-007	3.84e-016	4.5936e+003

Table B.9.: Glocke d10 h4.4 r7 r7

Mode	Frequency [Ghz]	$ (\mathbf{Ax}-\mathbf{x})/\mathbf{x} $	$\max(\mathbf{e})$	$\text{div}(\mathbf{e})$	Q-Factor
1	11.716058003	8.20e-005	6.69e-004	3.58e-015	3.7712e+003
2	16.1245244313	6.09e-005	3.10e-004	1.24e-015	4.1950e+003
3	16.124661173	2.50e-004	1.10e-003	6.40e-016	4.1978e+003
4	20.6801505821	1.80e-004	1.06e-003	3.32e-015	4.6414e+003
5	20.6805812525	3.63e-005	1.94e-004	3.64e-015	4.6318e+003
6	21.7480908013	2.43e-004	1.18e-003	2.01e-015	5.9397e+003
7	25.3222896234	5.62e-004	2.25e-003	6.03e-016	5.0015e+003
8	25.3223082439	2.60e-004	1.95e-003	8.16e-016	4.9999e+003
9	27.3635781257	5.21e-004	2.43e-003	3.06e-015	6.8896e+003
10	27.3636047292	4.72e-005	2.76e-004	2.66e-015	6.8977e+003
11	29.4124677714	1.04e-004	3.07e-004	1.78e-015	8.2526e+003
12	29.4124862068	3.59e-004	9.64e-004	1.74e-015	8.2603e+003
13	29.9674785074	4.86e-004	2.39e-003	7.83e-016	5.2974e+003
14	29.9685426194	6.54e-004	3.82e-003	1.06e-015	5.3318e+003

Table B.10.: Glocke d10 h4 r7 r5

Mode	Frequency [Ghz]	$ (\mathbf{Ax}-\mathbf{x})/\mathbf{x} $	$\max(\mathbf{e})$	$\text{div}(\mathbf{e})$	Q-Factor
1	11.591565068	5.26e-008	1.24e-006	4.31e-016	3.2295e+003
2	15.6903890011	7.43e-010	8.57e-009	4.30e-016	3.7303e+003
3	15.6905042905	9.83e-010	1.12e-008	4.24e-016	3.7313e+003
4	20.1952609468	3.62e-009	3.79e-008	1.96e-016	4.2541e+003
5	20.2041590705	2.49e-007	2.72e-006	4.04e-016	4.1916e+003
6	21.599474928	1.62e-008	1.09e-007	2.00e-016	5.6773e+003
7	24.8695114635	4.73e-008	5.96e-007	1.89e-016	4.6105e+003
8	24.8695593271	1.42e-008	9.03e-008	4.12e-016	4.6133e+003
9	27.5208934595	3.81e-007	4.17e-006	2.00e-016	6.3681e+003
10	27.5209552312	5.13e-008	9.20e-007	4.75e-016	6.4234e+003
11	29.5572014679	2.02e-008	2.24e-007	3.59e-016	4.9076e+003
12	29.5681466589	2.09e-008	1.62e-007	3.18e-016	4.9531e+003

Table B.11.: Glocke d12 h3 r4 r6 DE

Mode	Frequency [Ghz]	$ (\mathbf{Ax}-\mathbf{x})/\mathbf{x} $	$\max(\mathbf{e})$	$\text{div}(\mathbf{e})$	Q-Factor
1	9.77014391781	5.29e-009	2.22e-008	4.70e-016	3.2603e+003
2	13.4486158956	7.98e-007	6.84e-006	1.70e-016	3.7095e+003
3	13.4487328166	5.09e-008	1.70e-007	3.63e-016	3.7102e+003
4	17.3120292009	1.05e-007	3.11e-007	3.01e-016	3.8593e+003
5	17.3144722387	2.77e-007	7.41e-007	3.80e-016	3.8181e+003
6	19.1306940737	3.39e-007	8.76e-007	1.96e-016	4.3929e+003
7	20.9300179901	2.96e-007	1.25e-006	1.85e-016	3.6657e+003
8	20.9300216037	9.20e-007	2.78e-006	4.46e-016	3.6645e+003
9	23.4658555653	8.40e-007	2.76e-006	4.34e-016	3.6845e+003
10	23.46589433	9.13e-007	2.83e-006	3.18e-016	3.6838e+003
11	24.0926245254	7.65e-007	1.61e-006	1.85e-016	3.3428e+003
12	24.0927752357	8.29e-007	2.63e-006	3.28e-016	3.3452e+003

Table B.12.: Glocke d12 h4 r4 r6

Mode	Frequency [Ghz]	$ (\mathbf{Ax}-\mathbf{x})/\mathbf{x} $	$\max(\mathbf{e})$	$\text{div}(\mathbf{e})$	Q-Factor
1	11.5501430822	1.45e-008	2.33e-007	1.71e-016	3.1795e+003
2	15.5852368682	1.03e-009	3.89e-009	4.31e-016	3.6652e+003
3	15.5853861756	5.62e-011	1.21e-010	4.36e-016	3.6685e+003
4	20.1539554611	4.21e-008	3.94e-007	2.68e-016	4.1521e+003
5	20.1626952186	4.74e-008	4.21e-007	4.20e-016	4.0221e+003
6	21.7441540242	1.03e-007	1.62e-006	1.89e-016	5.5982e+003
7	24.8860673927	4.38e-008	6.35e-007	3.39e-016	4.4088e+003
8	24.8860948852	4.93e-008	6.71e-007	3.89e-016	4.3773e+003
9	27.5697567974	8.49e-008	9.69e-007	3.81e-016	5.9825e+003
10	27.5698613943	2.35e-007	2.84e-006	3.88e-016	6.0118e+003
11	29.6081029052	2.86e-008	1.92e-007	2.10e-016	4.7539e+003
12	29.6101679731	2.53e-007	1.78e-006	3.53e-016	4.4768e+003

Table B.13.: Glocke d12 h4 r6 r6

Mode	Frequency [Ghz]	$ (\mathbf{Ax}-\mathbf{x})/\mathbf{x} $	$\max(\mathbf{e})$	$\text{div}(\mathbf{e})$	Q-Factor
1	11.2974913957	2.19e-011	6.80e-010	2.96e-016	2.9604e+003
2	15.2800214905	5.75e-010	1.10e-008	3.17e-016	3.5335e+003
3	15.2801748333	1.51e-007	7.08e-007	3.33e-016	3.5397e+003
4	19.9794957739	2.08e-008	2.49e-007	3.15e-016	4.1204e+003
5	19.9886926841	5.64e-009	5.83e-008	3.22e-016	3.9241e+003
6	22.1137573932	5.30e-008	7.19e-007	1.92e-016	5.5746e+003
7	24.8077789382	5.53e-008	6.32e-007	3.92e-016	4.3841e+003
8	24.8077933842	8.91e-008	1.02e-006	4.06e-016	4.3912e+003
9	27.7244923647	5.06e-008	5.66e-007	2.03e-016	5.5066e+003
10	27.7245922606	4.84e-008	6.98e-007	3.39e-016	5.5031e+003


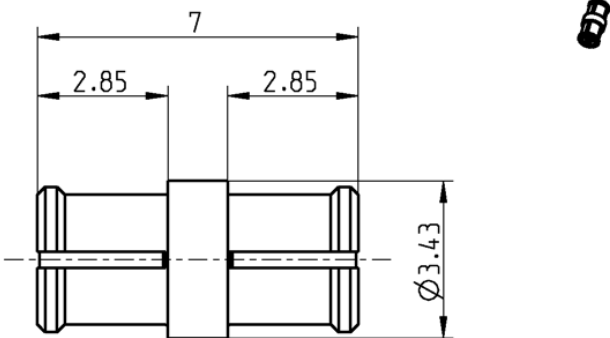
Table B.14.: Glocke d14 h4 r6 r15

Mode	Frequency [Ghz]	$ (\mathbf{Ax}-\mathbf{x})/\mathbf{x} $	max(e)	div(e)	Q-Factor
1	11.3504467559	3.80e-008	4.07e-007	3.76e-016	3.6632e+003
2	15.8137245397	3.64e-008	1.52e-007	4.23e-016	4.3601e+003
3	15.8154163075	4.41e-008	1.96e-007	4.14e-016	4.3552e+003
4	20.6009456612	9.85e-009	4.62e-008	3.91e-016	4.8465e+003
5	20.6153347422	5.79e-008	3.27e-007	3.40e-016	4.9611e+003
6	22.3701509905	6.29e-008	3.95e-007	1.78e-016	6.1228e+003
7	25.361296678	3.85e-008	2.21e-007	3.06e-016	5.3130e+003
8	25.3640658973	7.62e-007	4.81e-006	3.87e-016	5.3706e+003
9	27.742115373	5.78e-008	4.46e-007	4.85e-016	6.3941e+003
10	27.7454204592	1.09e-007	7.02e-007	3.04e-016	6.4747e+003

Table B.15.: 7Eck d24 d12 r

Mode	Frequency [Ghz]	$ (\mathbf{Ax}-\mathbf{x})/\mathbf{x} $	max(e)	div(e)	Q-Factor
1	12.3882113131	8.29e-007	1.29e-005	3.76e-016	3.2805e+003
2	16.8173745137	4.23e-010	3.36e-009	4.24e-016	3.7764e+003
3	16.8184976073	2.45e-009	3.94e-008	4.49e-016	3.7790e+003
4	21.7729665058	3.37e-009	3.76e-008	3.17e-016	4.3325e+003
5	21.7776786847	5.36e-007	7.99e-006	2.63e-016	4.1445e+003
6	23.5455463332	4.42e-008	5.10e-007	3.38e-016	5.7068e+003
7	26.7357091001	9.21e-008	7.08e-007	3.05e-016	4.5652e+003
8	26.7392720889	3.61e-008	2.73e-007	3.96e-016	4.5592e+003
9	29.2878041505	6.57e-008	1.01e-006	3.82e-016	5.8577e+003
10	29.2880127405	2.43e-007	1.89e-006	4.66e-016	5.9220e+003

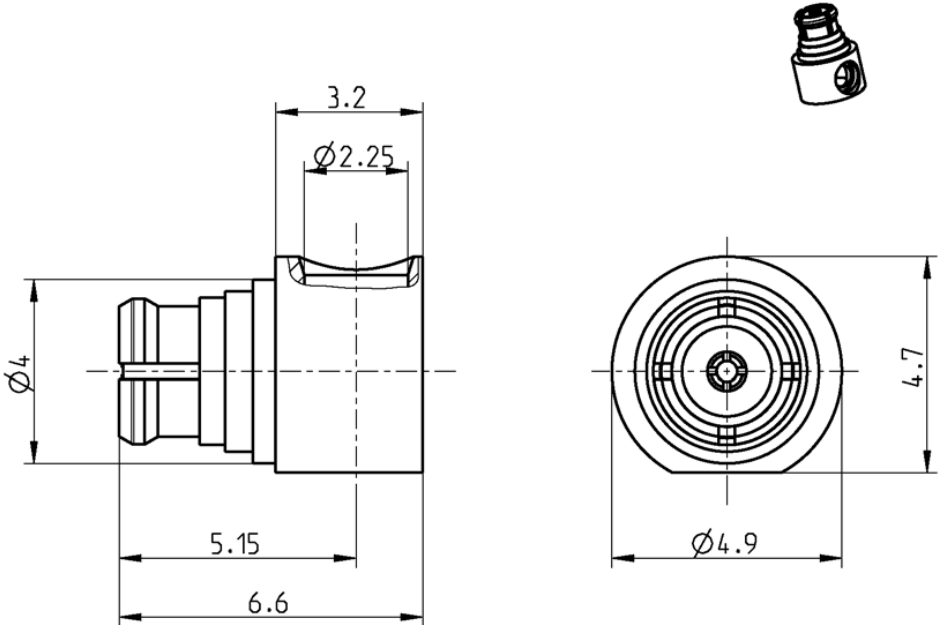
C. Rosenberger datasheets

TECHNICAL DATA SHEET														
ADAPTOR SMP JACK - JACK	19K102-K00L5													
<div style="text-align: center;">  </div> <p>All dimensions are in mm; tolerances acc. ISO 2768 m-H</p> <p>Interface According to MIL-STD-348A, Fig. 326</p> <p>Documents N/A</p> <p>Material and plating</p> <table border="0"> <thead> <tr> <th>Connector parts</th> <th>Material</th> <th>Plating</th> </tr> </thead> <tbody> <tr> <td>Center contact</td> <td>Beryllium copper</td> <td>Gold, min. 0.15 µm, over chemical nickel</td> </tr> <tr> <td>Outer contact</td> <td>Beryllium copper</td> <td>Gold, min. 0.15 µm, over chemical nickel</td> </tr> <tr> <td>Dielectric</td> <td>PTFE</td> <td></td> </tr> </tbody> </table>			Connector parts	Material	Plating	Center contact	Beryllium copper	Gold, min. 0.15 µm, over chemical nickel	Outer contact	Beryllium copper	Gold, min. 0.15 µm, over chemical nickel	Dielectric	PTFE	
Connector parts	Material	Plating												
Center contact	Beryllium copper	Gold, min. 0.15 µm, over chemical nickel												
Outer contact	Beryllium copper	Gold, min. 0.15 µm, over chemical nickel												
Dielectric	PTFE													
Rosenberger Hochfrequenztechnik GmbH & Co. KG P.O.Box 1260 D-84526 Tittmoning Germany www.rosenberger.de	Tel.: +49 8684 18-0 Fax: +49 8684 18-499 email: info@rosenberger.de	Page 1 / 2												


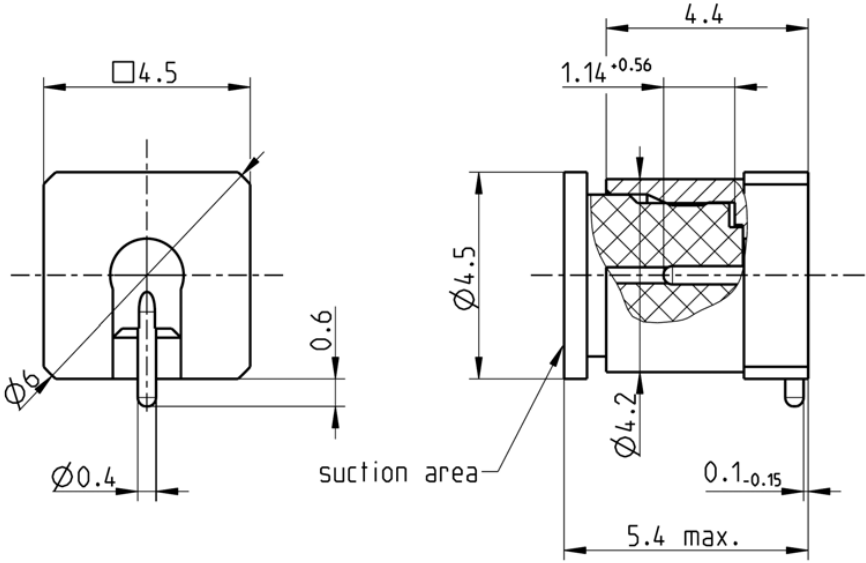
TECHNICAL DATA SHEET				Rosenberger®			
ADAPTOR SMP JACK - JACK				19K102-K00L5			
Electrical data							
Impedance	50 Ω						
Frequency	DC to 26.5 GHz						
Return loss	≥ 30 dB, DC to 10 GHz ≥ 15 dB, 10 to 18 GHz						
Insertion loss	≤ 0.1 x $\sqrt{f(\text{GHz})}$ dB, DC to 18 GHz						
Insulation resistance	≥ 5 GΩ						
Center contact resistance	≤ 6.0 mΩ						
Outer contact resistance	≤ 2.0 mΩ						
Test voltage	500 V rms						
Working voltage	335 V rms						
Contact Current	1.2A DC max.						
Mechanical data							
Mating cycles							
if mating part is smooth bore	≥ 1000						
if mating part is limited detent	≥ 500						
if mating part is full detent	≥ 100						
Center contact captivation	≥ 7 N						
Engagement force							
- smooth bore	9 N max.						
- limited detent	45 N max.						
- full detent	68 N max.						
Disengagement force							
- smooth bore	2.2 N min.						
- limited detent	9 N min.						
- full detent	22 N min.						
Environmental data							
Temperature range	-65°C to +155°C						
Thermal shock	MIL-STD-202, Method 107, Condition B						
Vibration	MIL-STD-202, Method 204, Condition B						
Shock	MIL-STD-202, Method 213, Condition A						
Moisture resistance	MIL-STD-202, Method 106						
2002/95/EC (RoHS)	compliant						
Tooling							
	N/A						
Suitable cables							
	N/A						
Packing							
Standard	100 pcs in bag						
Weight	0.2 g/pce						
<p>While the information has been carefully compiled to the best of our knowledge, nothing is intended as representation or warranty on our part and no statement herein shall be construed as recommendation to infringe existing patents. In the effort to improve our products, we reserve the right to make changes judged to be necessary.</p>							
Draft	Date	Approved	Date	Rev.	Engineering change number	Name	Date
F. Schmidhammer	06/04/06	Krautenbacher J.	26/09/06	b00	06-0478	B. Dandl	26/09/06
Rosenberger Hochfrequenztechnik GmbH & Co. KG P.O.Box 1260 D-84526 Tittmoning Germany www.rosenberger.de					Tel.: +49 8684 18-0 Fax: +49 8684 18-499 email: info@rosenberger.de		Page 2 / 2

TECHNICAL DATA SHEET		Rosenberger®													
SMP	BULKHEAD PLUG LIMITED DETENT	19S602-271L5													
<p>1) Panel piercing: $\varnothing 4.8^{+0.05}$ 2) Measured when retaining clip is fully pushed towards contact area.</p>															
<p>All dimensions are in mm; tolerances acc. ISO 2768 m-H</p>															
<p>Interface According to MIL-STD-348A, Fig. 326</p>															
<p>Documents Assembly instruction 19 E4</p>															
<p>Material and plating</p> <table border="0"> <thead> <tr> <th>Connector parts</th> <th>Material</th> <th>Plating</th> </tr> </thead> <tbody> <tr> <td>Center contact</td> <td>Brass</td> <td>AuroDur®, gold plated</td> </tr> <tr> <td>Outer contact</td> <td>Brass</td> <td>AuroDur®, gold plated</td> </tr> <tr> <td>Dielectric</td> <td>PTFE</td> <td></td> </tr> </tbody> </table>				Connector parts	Material	Plating	Center contact	Brass	AuroDur®, gold plated	Outer contact	Brass	AuroDur®, gold plated	Dielectric	PTFE	
Connector parts	Material	Plating													
Center contact	Brass	AuroDur®, gold plated													
Outer contact	Brass	AuroDur®, gold plated													
Dielectric	PTFE														
Rosenberger Hochfrequenztechnik GmbH & Co. KG P.O.Box 1260 D-84526 Tittmoning Germany www.rosenberger.de		Tel.: +49 8684 18-0 Fax: +49 8684 18-499 email: info@rosenberger.de	Page 1 / 2												

TECHNICAL DATA SHEET				Rosenberger®			
SMP		BULKHEAD PLUG LIMITED DETENT		19S602-271L5			
Electrical data							
Impedance				50 Ω			
Frequency				DC to 26.5 GHz			
Return loss				≥ 30 dB, DC to 4 GHz			
				≥ 20 dB, 4 to 12 GHz			
				≥ 18 dB, 12 to 26.5 GHz			
Insertion loss				≤ 0.05 x √f(GHz) dB, DC to 26.5 GHz			
Insulation resistance				≥ 5 GΩ			
Center contact resistance				≤ 6.0 mΩ			
Outer contact resistance				≤ 2.0 mΩ			
Test voltage				500 V rms			
Working voltage				335 V rms			
Contact Current				1.2A DC max.			
<i>- Limitations are possible due to the used cable type -</i>							
Mechanical data							
Mating cycles				≥ 500			
Center contact captivation:				≥ 7 N			
Engagement force							
- limited detent				45 N max.			
Disengagement force							
- limited detent				9 N min.			
Environmental data							
Temperature range				-65°C to +155°C			
Thermal shock				MIL-STD-202, Method 107, Condition B			
Vibration				MIL-STD-202, Method 204, Condition B			
Shock				MIL-STD-202, Method 213, Condition A			
Moisture resistance				MIL-STD-202, Method 106			
2002/95/EC (RoHS)				compliant			
Tooling							
			N/A				
Suitable cables							
			RG 405 /U, UT 85-M17				
Packing							
Standard				100 pcs in bag			
Weight				1.04 g/pce			
<p>While the information has been carefully compiled to the best of our knowledge, nothing is intended as representation or warranty on our part and no statement herein shall be construed as recommendation to infringe existing patents. In the effort to improve our products, we reserve the right to make changes judged to be necessary.</p>							
Draft	Date	Approved	Date	Rev.	Engineering change number	Name	Date
Inge Mühlauer	17/08/04	A. König	26/09/07	c00	07-0154	S. Huber-Siegl	26/09/07
Rosenberger Hochfrequenztechnik GmbH & Co. KG P.O.Box 1260 D-84526 Tittmoning Germany www.rosenberger.de				Tel.: +49 8684 18-0 Fax: +49 8684 18-499 email: info@rosenberger.de			Page 2 / 2

TECHNICAL DATA SHEET	Rosenberger®													
SMP RIGHT ANGLE JACK	19K202-271L5													
 <p>All dimensions are in mm; tolerances acc. ISO 2768 m-H</p> <p>Interface According to MIL-STD-348A, Fig. 326</p> <p>Documents Assembly instruction 19 E8</p> <p>Material and plating</p> <table border="0" style="width: 100%;"> <tr> <td style="width: 33%;">Connector parts</td> <td style="width: 33%;">Material</td> <td style="width: 33%;">Plating</td> </tr> <tr> <td>Center contact</td> <td>CuBe</td> <td>AuroDur®, gold plated</td> </tr> <tr> <td>Outer contact</td> <td>CuBe</td> <td>AuroDur®, gold plated</td> </tr> <tr> <td>Dielectric</td> <td>PTFE</td> <td></td> </tr> </table>			Connector parts	Material	Plating	Center contact	CuBe	AuroDur®, gold plated	Outer contact	CuBe	AuroDur®, gold plated	Dielectric	PTFE	
Connector parts	Material	Plating												
Center contact	CuBe	AuroDur®, gold plated												
Outer contact	CuBe	AuroDur®, gold plated												
Dielectric	PTFE													
Rosenberger Hochfrequenztechnik GmbH & Co. KG P.O.Box 1260 D-84526 Tittmoning Germany www.rosenberger.de	Tel.: +49 8684 18-0 Fax: +49 8684 18-499 email: info@rosenberger.de	Page 1 / 2												

TECHNICAL DATA SHEET				Rosenberger®			
SMP RIGHT ANGLE JACK				19K202-271L5			
Electrical data							
Impedance	50 Ω						
Frequency	DC to 26.5 GHz						
Return loss	≥ 26 dB, DC to 6 GHz ≥ 20 dB, 6 to 12 GHz ≥ 16 dB, 12 to 26.5 GHz						
Insertion loss	≤ 0.1 x $\sqrt{f(\text{GHz})}$ dB						
Insulation resistance	≥ 5 GΩ						
Center contact resistance	≤ 6.0 mΩ						
Outer contact resistance	≤ 2.0 mΩ						
Test voltage	500 V rms						
Working voltage	335 V rms						
Contact Current	1.2A DC max.						
<i>- Limitations are possible due to the used cable type -</i>							
Mechanical data							
Mating cycles							
if mating part is smooth bore	≥ 1000						
if mating part is limited detent	≥ 500						
if mating part is full detent	≥ 100						
Center contact captivation	≥ 7 N						
Engagement force							
- smooth bore	9 N max.						
- limited detent	45 N max.						
- full detent	68 N max.						
Disengagement force							
- smooth bore	2.2 N min.						
- limited detent	9 N min.						
- full detent	22 N min.						
Environmental data							
Temperature range	-65°C to +155°C						
Thermal shock	MIL-STD-202, Method 107, Condition B						
Vibration	MIL-STD-202, Method 204, Condition B						
Shock	MIL-STD-202, Method 213, Condition A						
Moisture resistance	MIL-STD-202, Method 106						
2002/95/EC (RoHS)	compliant						
Tooling							
	N/A						
Suitable cables							
	UT 85, RG 405						
Packing							
Standard	500 pcs in bag						
Weight	0.5 g/pce						
<p>While the information has been carefully compiled to the best of our knowledge, nothing is intended as representation or warranty on our part and no statement herein shall be construed as recommendation to infringe existing patents. In the effort to improve our products, we reserve the right to make changes judged to be necessary.</p>							
Draft	Date	Approved	Date	Rev.	Engineering change number	Name	Date
Inge Mühlauer	17/08/04	Gramsamer J.	13/07/07	d00	07-0154	Gramsamer J.	13/07/07
Rosenberger Hochfrequenztechnik GmbH & Co. KG P.O.Box 1260 D-84526 Tittmoning Germany www.rosenberger.de					Tel.: +49 8684 18-0 Fax: +49 8684 18-499 email: info@rosenberger.de		Page 2 / 2

TECHNICAL DATA SHEET		Rosenberger	
SMP	STRAIGHT PLUG PCB LIMITED DETENT, SMD	19S102-40ML5	
			
			
All dimensions are in mm; tolerances acc. ISO 2768 m-H			
Interface			
Similar to		MIL-STD-348A, Fig. 326	
Documents			
PCB layout		please request optimized footprint for your application	
Tape & reel packaging		VG01.01M00	
Material and plating			
Connector parts		Material	Plating
Center contact		Beryllium copper	AuroDur, gold plated
Outer contact		Brass	AuroDur, gold plated
Dielectric		Casting resin	
Rosenberger Hochfrequenztechnik GmbH & Co. KG P.O.Box 1260 D-84526 Tittmoning Germany www.rosenberger.de		Tel.: +49 8684 18-0 Fax: +49 8684 18-499 email: info@rosenberger.de	Page 1 / 2

TECHNICAL DATA SHEET				Rosenberger			
SMP		STRAIGHT PLUG PCB LIMITED DETENT, SMD		19S102-40ML5			
Electrical data							
Impedance	50 Ω						
Frequency	DC to 40 GHz						
Return loss	≥ 26 dB, DC to 12 GHz ≥ 17 dB, 12 to 40 GHz						
Insertion loss	≤ 0.05 x √f(GHz) dB						
Insulation resistance	≥ 5 GΩ						
Center contact resistance	≤ 6.0 mΩ						
Outer contact resistance	≤ 2.0 mΩ						
Test voltage	500 V rms						
Working voltage	335 V rms						
Contact Current	1.2A DC max.						
- VSWR in application depends decisive on PCB layout -							
Mechanical data							
Mating cycles	≥ 500						
Center contact captivation	≥ 7 N						
Engagement force	45 N max.						
- limited detent							
Disengagement force	9 N min.						
- limited detent							
Environmental data							
Temperature range	-65°C to +155°C						
Thermal shock	MIL-STD-202, Method 107, Condition B						
Vibration	MIL-STD-202, Method 204, Condition B						
Shock	MIL-STD-202, Method 213, Condition A						
Moisture resistance	MIL-STD-202, Method 106						
Max. soldering temperature	IEC 61760-1, +260°C for 10 sec.						
2002/95/EC (RoHS)	compliant						
Tooling							
N/A							
Suitable cables							
N/A							
Packing							
Standard	1500 pcs in tape & reel, B1500T 100 pcs in blister, B0100B						
Weight	0.41 g/pce						
While the information has been carefully compiled to the best of our knowledge, nothing is intended as representation or warranty on our part and no statement herein shall be construed as recommendation to infringe existing patents. In the effort to improve our products, we reserve the right to make changes judged to be necessary.							
Draft	Date	Approved	Date	Rev.	Engineering change number	Name	Date
Inge Mühlauer	14/03/05	T. Höher	07/06/10	g00	10-0394	S_Krautenb.	07.06.10
Rosenberger Hochfrequenztechnik GmbH & Co. KG P.O.Box 1260 D-84526 Tittmoning Germany www.rosenberger.de				Tel.: +49 8684 18-0 Fax: +49 8684 18-499 email: info@rosenberger.de			Page 2 / 2

D. Rogers datasheet



Advanced Circuit Materials

Advanced Circuit Materials
 100 S. Roosevelt Avenue
 Chandler, AZ 85226
 Tel: 480-961-1382, Fax: 480-961-4533
www.rogerscorporation.com

Data Sheet

TM1.1000

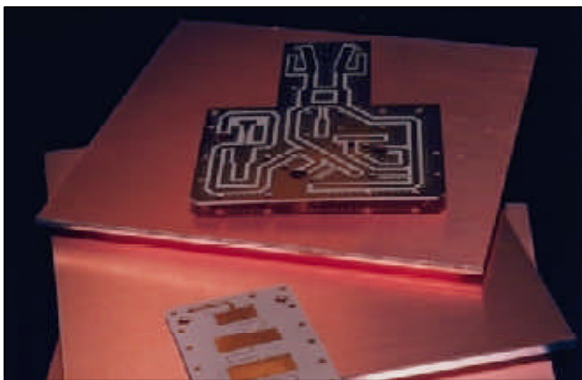
TMM® Temperature Stable Microwave Laminate

Features:

- Wide range of dielectric constants. Ideal for single material systems on a wide variety of applications.
- Excellent mechanical properties versus temperature. Resists creep and cold flow. Reliable in severe thermal stress environments.
- Exceptionally low thermal coefficient of dielectric constant. Consistent electrical performance over temperature ranges.
- Coefficient of thermal expansion matched to copper. High reliability of plated through holes.
- Resistant to process chemicals. No damage to material during fabrication and assembly processes.
- Thermoset resin for reliable wirebonding. No specialized production techniques required. TMM 10 and 10i laminates can replace alumina substrates.

Some Typical Applications:

- RF and Microwave Circuitry
- Global Positioning System Antennas
- Power Amplifiers and Combiners
- Patch Antennas
- Temperature Stable Filters and Couplers
- Dielectric Polarizers and Lenses
- Satellite Communication Systems
- Chip Testers



TMM® Temperature Stable Microwave laminates are ceramic thermoset polymer composites designed for high reliability stripline and microstrip applications. TMM laminates are available in a wide range of dielectric constants and claddings.

The electrical and mechanical properties of TMM laminates combine many of the benefits of both ceramic and traditional PTFE microwave circuit laminates, without requiring the specialized production techniques common to these materials. TMM laminates do not require a sodium naphthanate treatment prior to electroless plating.

An exceptionally low thermal coefficient of dielectric constant, typically less than 30 ppm/C, results in consistent electrical performance over broad temperature ranges.

TMM laminates have isotropic coefficients of thermal expansion, very closely matched to copper, allowing for production of high reliability plated through holes, and low etch shrinkage values. Furthermore, the thermal conductivity of TMM laminates is approximately twice that of traditional PTFE/ceramic laminates, facilitating heat removal.

TMM laminates are based on thermoset resins, and do not soften when heated. As a result, wire bonding of component leads to circuit traces can be performed without concerns of pad lifting or substrate deformation.

TMM laminates combine many of the desirable features of ceramic substrates with the ease of soft substrate processing techniques. TMM temperature stable microwave laminates are available clad with 1/4 oz/ft² to 2 oz/ft² (8 to 70µm) electrodeposited copper foil, or bonded directly to brass or aluminum plates. Substrate thicknesses of 0.015" to 0.500" and greater are available. The base substrate is resistant to etchants and solvents used in printed circuit production. Consequently, all common PWB processes can be used to produce TMM microwave laminates.

The world runs better with Rogers.

PROPERTIES	TYPICAL VALUES					DIRECTION	UNITS	CONDITION	METHOD
	TMM 3	TMM 4	TMM 6	TMM 10	TMM 10I				
Dielectric Constant, ϵ_r	3.27± 0.032	4.50± 0.045	6.00± 0.080	9.20± 0.230	9.80± 0.245	Z	—	10 GHz	IPC-TM-650 Method 2.5.5.5
Dissipation Factor $\tan \delta$	0.0020	0.0020	0.0023	0.0022	0.0020	Z	—	10 GHz	IPC-TM-650 Method 2.5.5.5
Thermal Coefficient of ϵ_r	+37	+14*	-11	-38	-43*		ppm/K	-55 +125°C	IPC-TM-650 Method 2.5.5.5
Insulation Resistance	>2000	>2000	>2000	>2000	>2000		Gohm	C96/60/95	ASTM D257
Volume Resistivity	3 X 10 ⁹	6 X 10 ⁸	1 X 10 ⁸	2 X 10 ⁷	—		Mohm•cm		ASTM D257
Surface Resistivity	>9 X 10 ⁹	1 X 10 ⁹	1 X 10 ⁸	4 X 10 ⁷	—		Mohm		ASTM D257
Flexural Strength	16.53	15.91	15.02	13.62	—	X,Y	kpsi	A	ASTM D790
Flexural Modulus	1.72	1.76	1.75	1.79	1.80*	X,Y	Mpsi	A	ASTM D790
Impact, Notch Izod	0.33	0.36	0.42	0.43	—	X,Y	ft-lb/in		ASTM D256A
Water Absorption (2 X 2") 3.18 mm (0.125") thk 1.27 mm (0.050) thk	0.06 0.12	0.07 0.18	0.06 0.20	0.09 0.20	0.16 0.13		%	D48/50	ASTM D570
Specific Heat	0.87	0.83	0.78	0.74	0.72*		J/g/K	A	Calculated
Thermal Conductivity	0.70	0.70	0.72	0.76	0.76	Z	W/m/K	80°C	ASTM C518
Thermal Expansion	15 23	16 21	18 26	21 20	19 20	X,Y Z	ppm/K	0 to 140°C	ASTM D3386
Density	1.78	2.07	2.37	2.77	2.77			A	ASTM D792
Copper Peel Strength	3.0	3.0	3.0	3.0	3.0	X,Y	lb/inch	after solder float 1oz. EDC	IPC-TM-650 Method 2.4.8

*estimated

AVAILABLE THICKNESS:		STANDARD PANEL SIZE:	STANDARD COPPER CLADDING:
0.015" (0.381mm)	0.125" (3.175mm)	18" X 12" (457 X 305mm)	¼ oz. (8 µm), ½ oz. (17µm), 1 oz. (35µm), 2 oz. (70µm) electrodeposited copper foil. Heavy cladding available. Contact Rogers Customer Service.
0.020" (0.508mm)	0.150" (3.810mm)	18" X 24" (457 X 610mm)	
0.025" (0.635mm)	0.200" (5.080mm)		
0.030" (0.762mm)	0.250" (6.350mm)		
0.050" (1.270mm)	0.275" (6.985mm)		
0.060" (1.524mm)	0.300" (7.620mm)		
0.075" (1.905mm)	0.500" (12.70mm)		
0.100" (2.540mm)			

CONTACT INFORMATION:

USA:	Rogers Advanced Circuit Materials, ISO 9002 Certified	Tel: 480-961-1382	Fax: 480-961-4533
Belgium:	Rogers N.V.	Tel: +32-9-2353611	Fax: +32-9-2353658
Japan:	Rogers Japan Inc.	Tel: 81-3-5200-2700	Fax: 81-3-5220-0571
Taiwan:	Rogers Taiwan Inc.	Tel: 886-2-86609056	Fax: 886-2-86609057
Korea:	Rogers Korea Inc.	Tel: 82-31-716-6112	Fax: 82-31-716-6208
Singapore:	Rogers Technologies Singapore Inc.	Tel: 65-747-3521	Fax: 65-747-7425

The information in this data sheet is intended to assist you in designing with Rogers laminates. It is not intended to and does not create any warranties express or implied, including any warranty of merchantability or fitness for a particular application. The user should determine the suitability of Rogers laminates for each application.

These commodities, technology or software are exported from the United States in accordance with the Export Administration regulations. Diversion contrary to U.S. law prohibited.

TMM® is a licensed trademark of Rogers Corporation.
© 1999-2002 Rogers Corporation, Printed in U.S.A.
0613-0202-5.0-ON
Publication # 92-108

E. Eccosorb datasheet



RoHS
Compliant

ECCOSORB® CR

Two-Part Castable Load Absorber Series

Material Characteristics

- Castable epoxy resin that remains rigid when cured
- ECCOSORB® CR will duplicate the physical and electrical properties of its counterpart in the ECCOSORB® MF series. For example, ECCOSORB® CR-117 is the equivalent to ECCOSORB® MF-117
- Frequency range from 1 - 18 GHz
- Dark Gray in color
- Low out-gassing properties for space applications

Applications

- ECCOSORB® CR can be used to mold waveguide terminations, attenuators, and loads to size
- ECCOSORB® CR can also be used to precisely pot small amounts of absorber in or around areas of RF leakage

Shipping & Availability

- ECCOSORB® CR is available in six castable versions, CR-110, CR-112, CR-114, CR-116, CR-117, & CR-124
- ECCOSORB® CR is supplied as a two part system consisting of a Component X and Component Y in 2 pound (quart) and 5 pound (gallon) kits
- Both CR-117 and CR-124 are available in premixed and frozen 5cc, 10cc, and 30cc syringes. No Mixing is needed. Note: Premixed and frozen packaging requires storage at -40°F (-40°C) and shelf life is 3 months. Minimum buy is 100 syringes for any size.
- Component Y ships as a hazardous material: Class 6.1, UN1673, P/G III

Instructions for Use

- Prepare mold by applying a thin coat of butchers wax
- Mix Part X in its shipping container to a uniform consistency before removing any material
- If crystals appear in Part Y, gently heat to 150 °F until crystals go into solution
- Weigh out the desired amounts of both Part X and Part Y in accordance with the table at right
- Heat Part X to about 150 °F. This will reduce the viscosity substantially and improve pourability. Note: in an effort to drop viscosity do not dilute with any chemical as this would alter the electrical performance of the material
- Thoroughly blend Part X and Part Y. Remove entrapped air, if necessary, by vacuum evacuation
- Pour into mold (pot life at 150 °F is about 1 hour) and cure per the below schedule. The mold is also preferably preheated to about 150 °F
- Clean up can be done with a solvent such as MEK

Typical Properties

Service Temperature, °F (°C)	<356 (<180)
Specific Gravity	1.6 to 4.6
Thermal Expansion Coefficient (°C)	30 x 10 ⁻⁶
Izod Impact, ft-lb/in of notch (ergs/cm)	0.3 (1.6 x 10 ⁶)
Water Absorption, %, 7 days immersion	0.1
Flexural Strength, psi (kg/cm ²)	15,000 (1050)
%TML	0.08 - 0.51
%CVCM	0.001 - 0.01
Shelf Life at temp. no higher than 77 °F	6 months

Recommended Frequency and Mixing Ratios by Weight

Series	Range (GHz)	Part X	Part Y
CR-110	26+	100	12.0
CR-112	12 - 18	100	8.2
CR-114	10 - 14	100	4.8
CR-116	6 - 12	100	3.0
CR-117	4 - 8	100	2.3
CR-124	5 and below	100	2.0

Recommended Cure Schedule

Temperature	Cure Time
165°F (74°C)	12 hours
200°F (93°C)	4 hours
250°F (121°C)	2 hours
300°F (149°C)	1 hour

EMERSON & CUMING MICROWAVE PRODUCTS, INC., 28 York Avenue, Randolph, MA 02368 / Telephone (781) 961-9600. Use of Information and Material: Values shown are based on testing of laboratory test specimens and represent data that falls within normal range of the material. These values are not intended for use in establishing maximum, minimum or ranges of values for specification purposes. Any determination of the suitability of the material for any purpose contemplated by the user and the manner of such use is the responsibility of the user. The user should determine that the material meets the needs of the user's product and use. We hope that the information given here will be helpful. It is based on data and knowledge considered to be true and accurate and is offered for the user's consideration, investigation and verification but we do not warrant the results to be obtained. Please read all statements, recommendations or suggestions in conjunction with our conditions of sale INCLUDING THOSE LIMITING WARRANTIES AND REMEDIES, which apply to all goods supplied by us. We assume no responsibility for the use of these statements, recommendations or suggestions nor do we intend them as a recommendation for any use, which would infringe any patent or copyright. Emerson & Cuming Microwave Products Inc.

Revision: 10/8/2008

www.eccosorb.com

A23



Typical Attenuation

	GHz	10 ⁻⁷	10 ⁻⁶	10 ⁻⁵	10 ⁻⁴	10 ⁻³	10 ⁻²	10 ⁻¹	1.0	3.0	8.6	10.0	18.0
CR-110	dB/cm	0	0	0	0	0	0	0.01	0.09	0.26	2.0	2.2	6.6
	dB/in	0	0	0	0	0	0	0.03	0.23	0.66	5.0	5.6	17
CR-112	dB/cm	0	0	0	0	0	0	0.02	0.16	0.59	4.9	5.6	10.1
	dB/in	0	0	0	0	0	0	0.05	0.41	1.5	12.4	14.2	25.7
CR-114	dB/cm	0	0	0	0	0	0	0.04	0.57	2.2	10.8	13.2	24.9
	dB/in	0	0	0	0	0	0	0.10	1.4	5.6	27.4	33.5	63.2
CR-116	dB/cm	0	0	0	0	0	0	0.09	1.3	5.0	21	32	57
	dB/in	0	0	0	0	0	0	0.23	3.3	12.7	53	81	145
CR-117	dB/cm	0	0	0	0	0	0.03	0.27	2.8	11	46	56	119
	dB/in	0	0	0	0	0	0.08	0.69	7.1	28	117	142	302
CR-124	dB/cm	0	0	0	0	0	0.03	0.48	6.5	20	63	67	149
	dB/in	0	0	0	0	0	0.08	1.2	16.51	50	160	170	378

*Note: Attenuation is a theoretical property calculated from the Complex Permittivity and Complex Permeability of a lossy material and is strictly a means of comparing one absorbing material to another. The attenuation properties are not an indication of how the material will perform inside a microwave device. For further electrical and physical properties of the ECCOSORB® CR series, please see the Typical Electrical Properties Table on the ECCOSORB® MF technical bulletin

EMERSON & CUMING MICROWAVE PRODUCTS, INC., 28 York Avenue, Randolph, MA 02368 / Telephone (781) 961-9600. Use of Information and Material: Values shown are based on testing of laboratory test specimens and represent data that falls within normal range of the material. These values are not intended for use in establishing maximum, minimum or ranges of values for specification purposes. Any determination of the suitability of the material for any purpose contemplated by the user and the manner of such use is the responsibility of the user. The user should determine that the material meets the needs of the user's product and use. We hope that the information given here will be helpful. It is based on data and knowledge considered to be true and accurate and is offered for the user's consideration, investigation and verification but we do not warrant the results to be obtained. Please read all statements, recommendations or suggestions in conjunction with our conditions of sale INCLUDING THOSE LIMITING WARRANTIES AND REMEDIES, which apply to all goods supplied by us. We assume no responsibility for the use of these statements, recommendations or suggestions nor do we intend them as a recommendation for any use, which would infringe any patent or copyright. Emerson & Cuming Microwave Products Inc.

Revision: 10/8/2008

www.eccosorb.com

A23

F. Transmission measurements

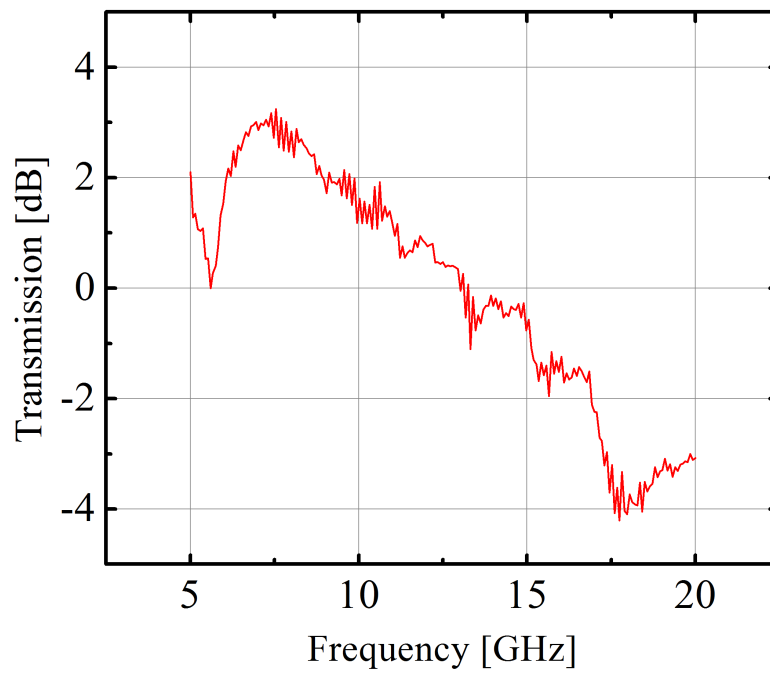


Figure F.18.: Transmission of connected cables

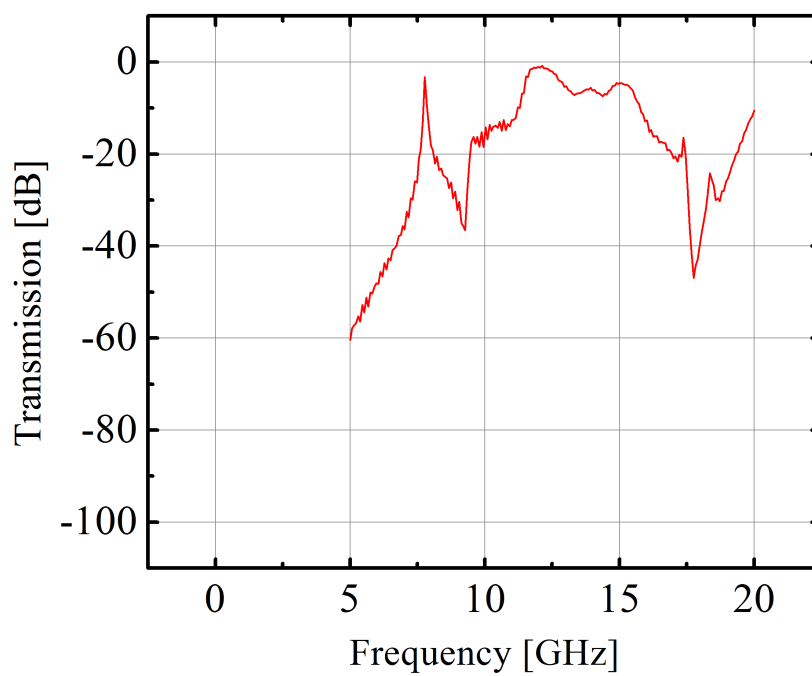


Figure F.19.: Transmission of the old sample holder

F.1. Transmission in the bell shaped cavity

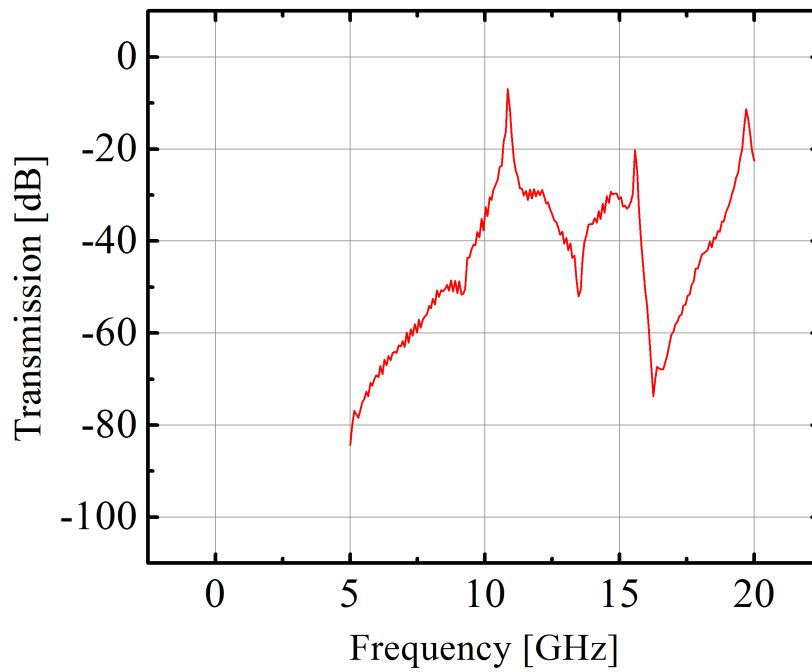


Figure F.20.: Bellshaped cavity, plugs in positions 1 and 2, bores taped

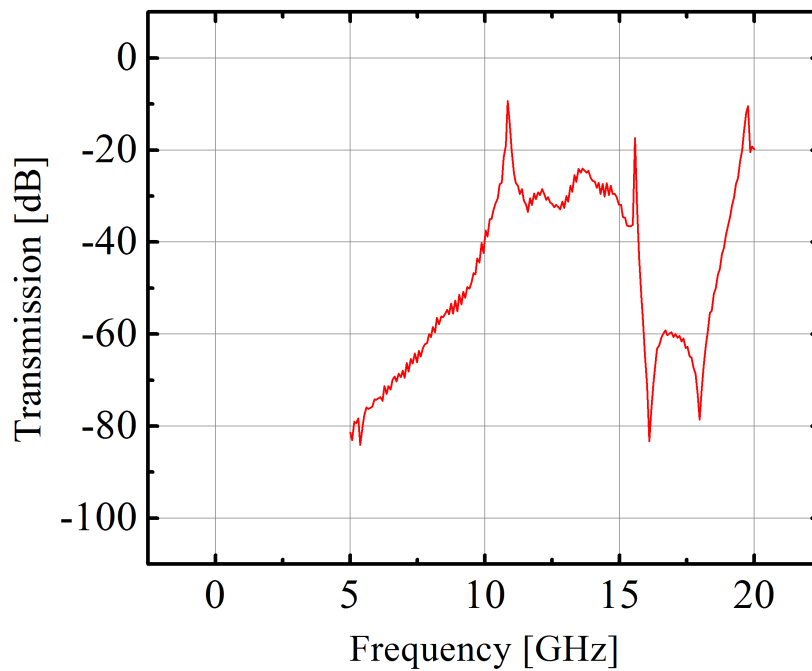


Figure F.21.: Bellshaped cavity, plugs in positions 1 and 3

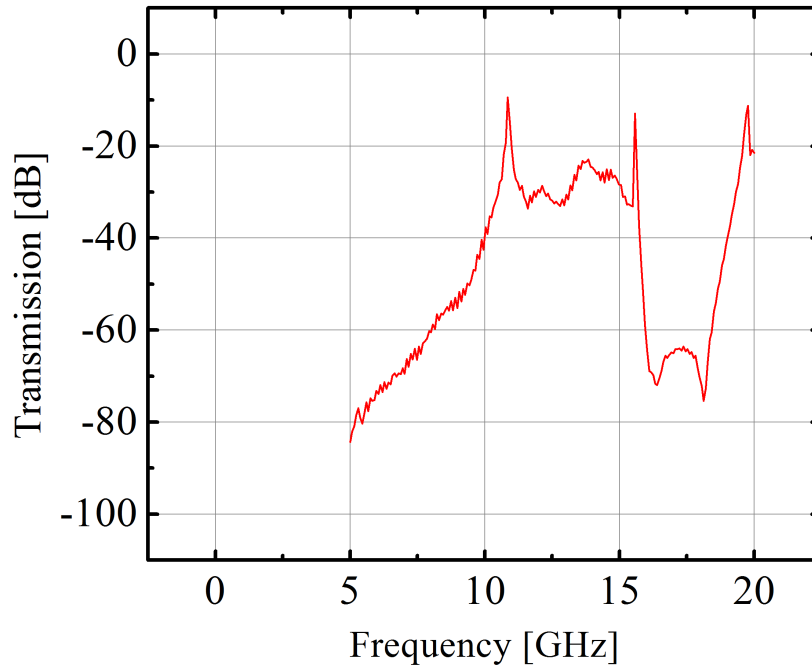


Figure F.22.: Bellshaped cavity, plugs in positions 1 and 3, bores taped

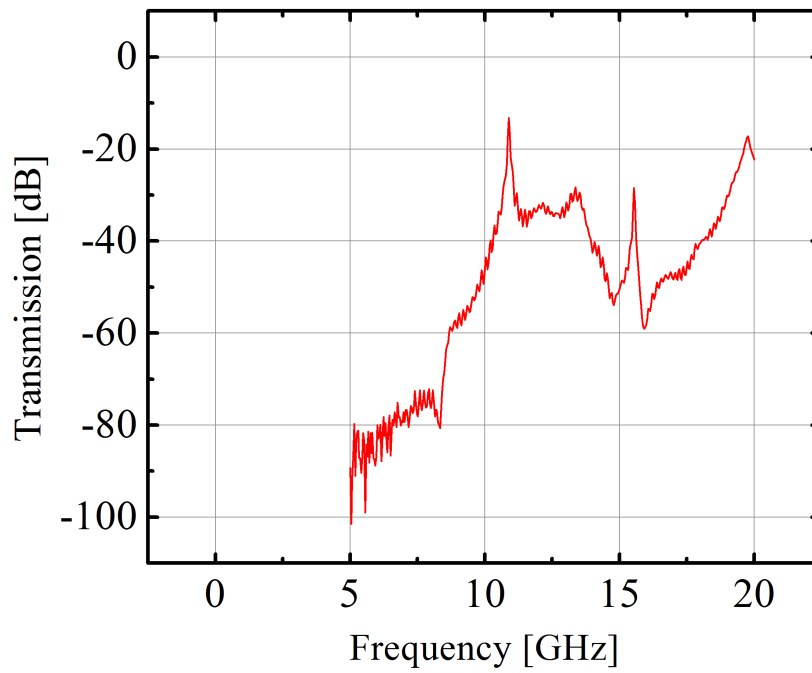


Figure F.23.: Bellshaped cavity, plugs in positions 1 and 4

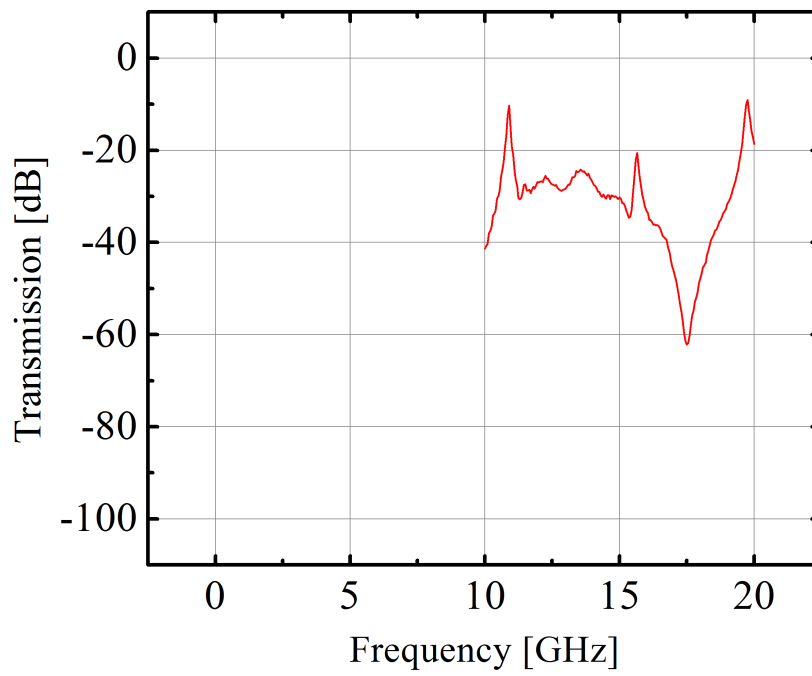


Figure F.24.: Bellshaped cavity, plugs in positions 1 and 4, bores taped

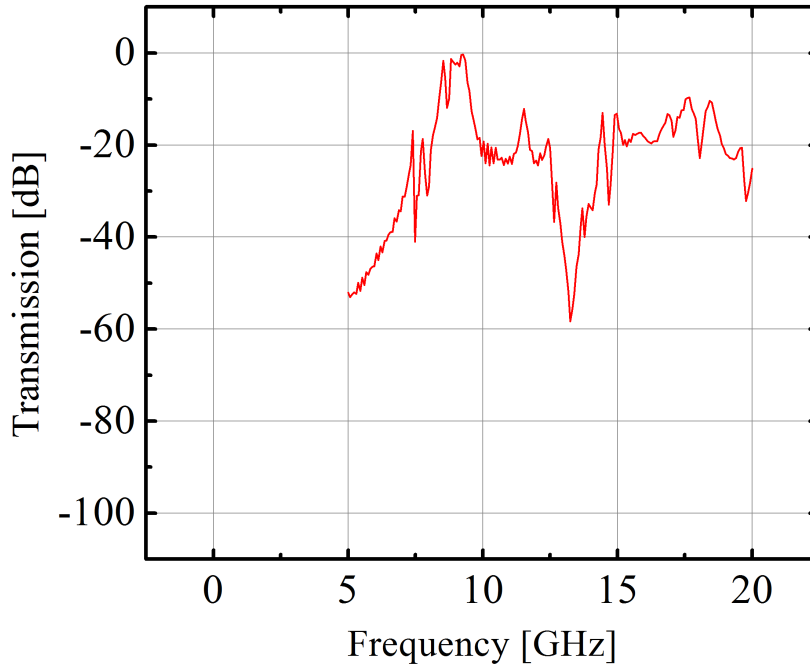
F.2. Transmission in the bell shaped cavity with PCB

Figure F.25.: Bellshaped cavity, plugs in positions 1 and 2, with PCB

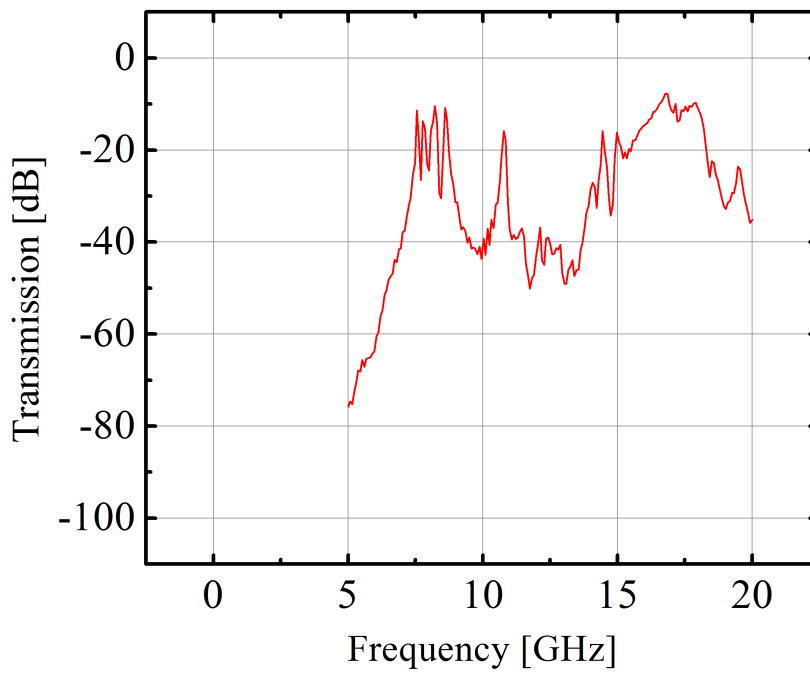


Figure F.26.: Bellshaped cavity, plugs in positions 1 and 3, with PCB

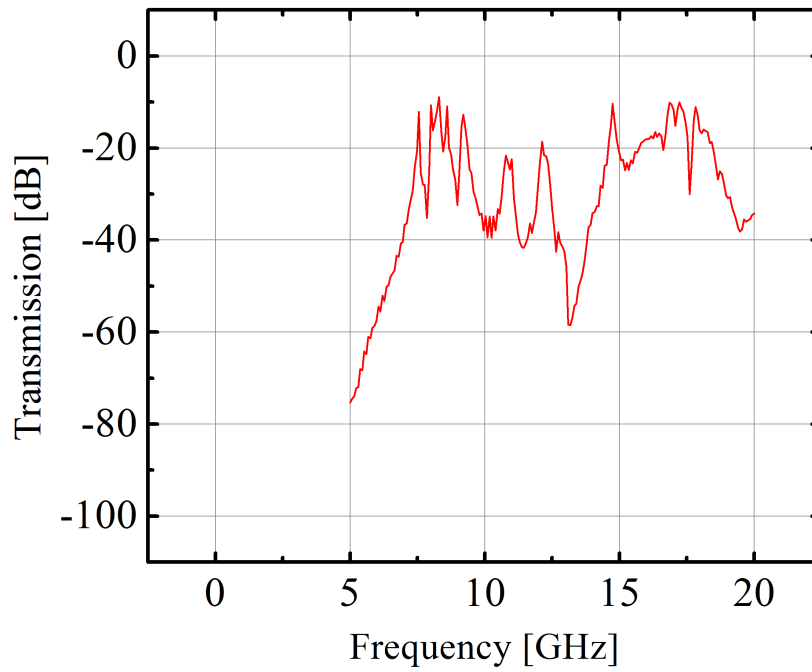


Figure F.27.: Bellshaped cavity, plugs in positions 1 and 4, with PCB

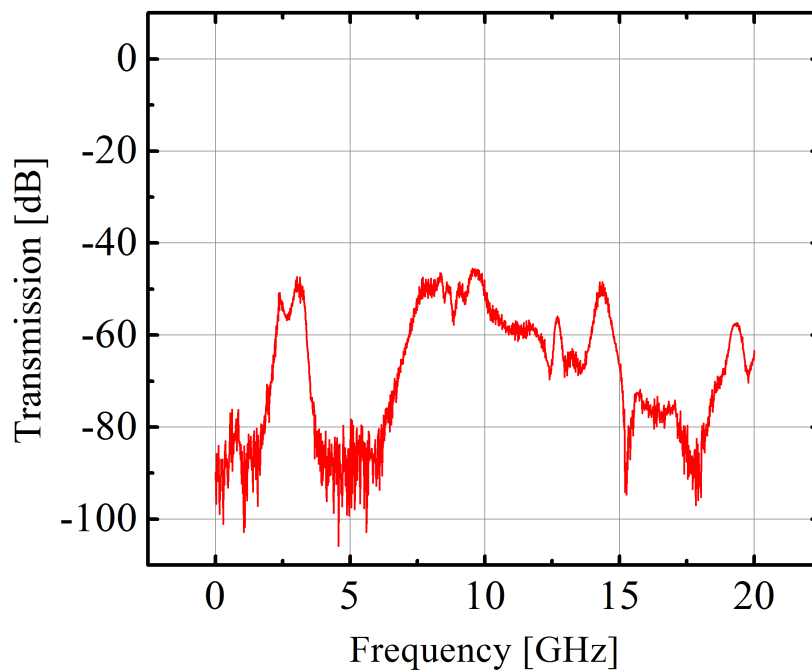


Figure F.28.: Bellshaped cavity, plugs in positions 1 and 4, with PCB and Eccosorb

F.3. Transmission in the new sample holder

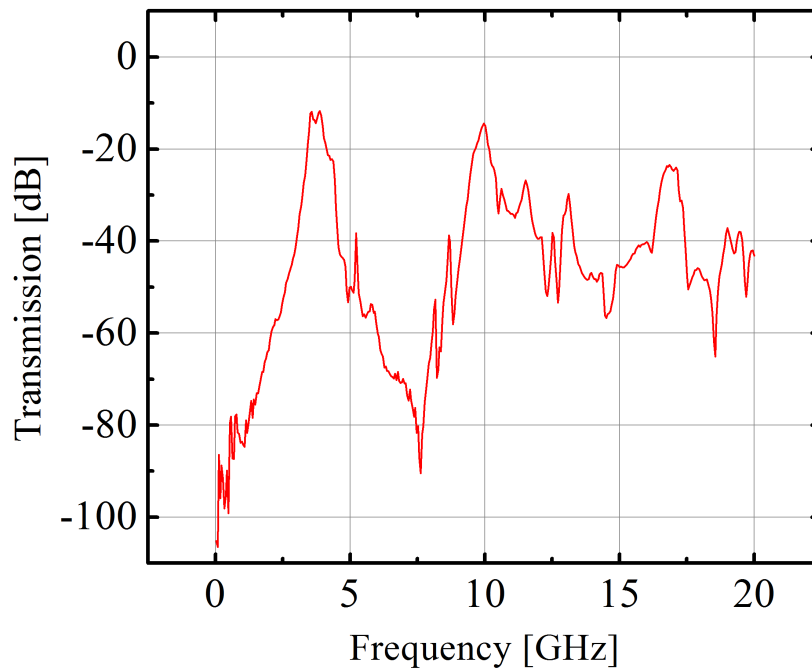


Figure F.29.: Small cylindrical cavity, plugs in positions 1 and 4, with PCB

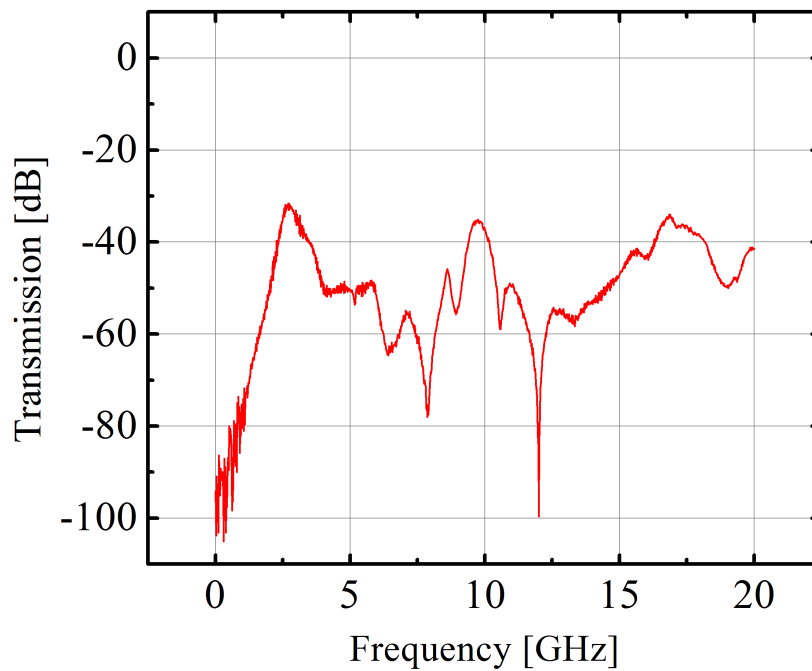


Figure F.30.: Small cylindrical cavity, plugs in positions 1 and 4, with PCB and Eccosorb

F.4. Transmissionrates compared

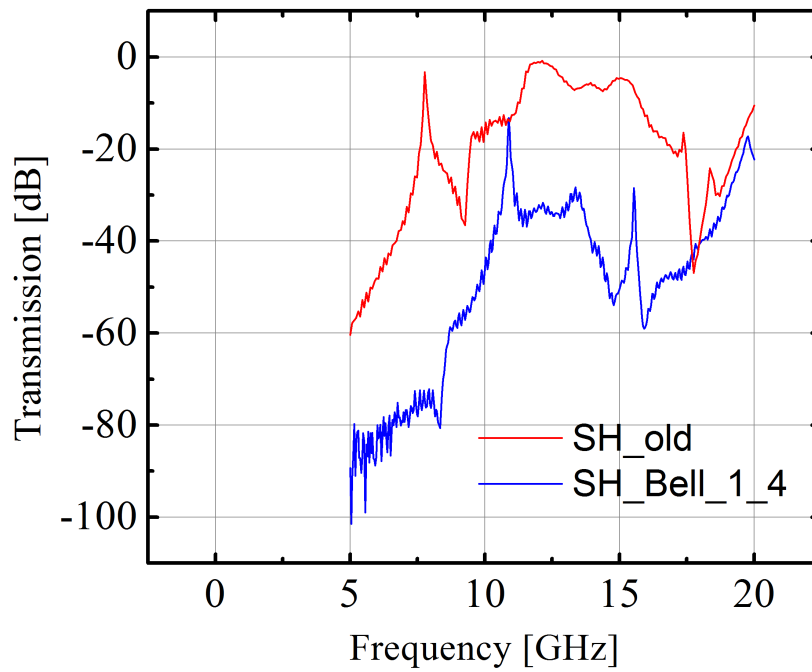


Figure F.31.: Old sample holder and bellshaped cavity, no PCB

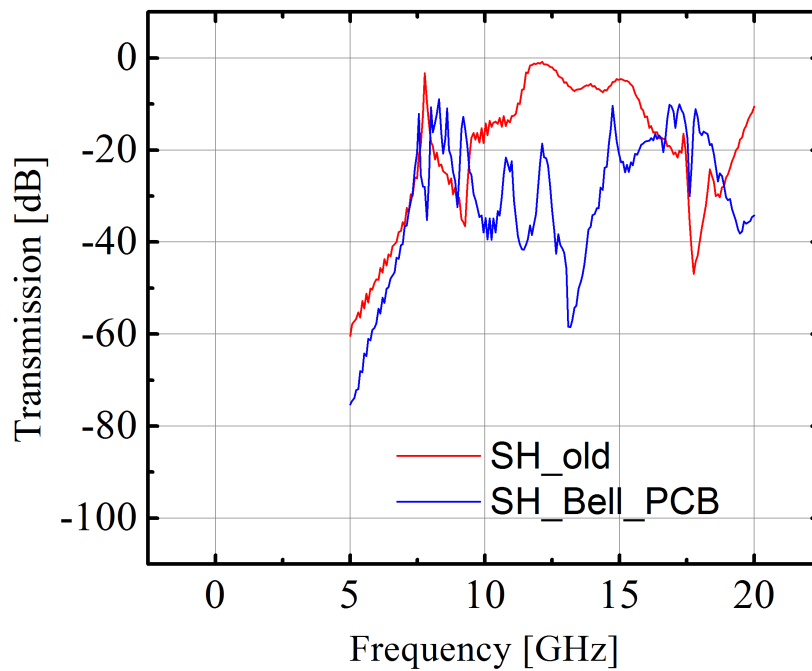


Figure F.32.: Old sample holder and bellshaped cavity with PCB

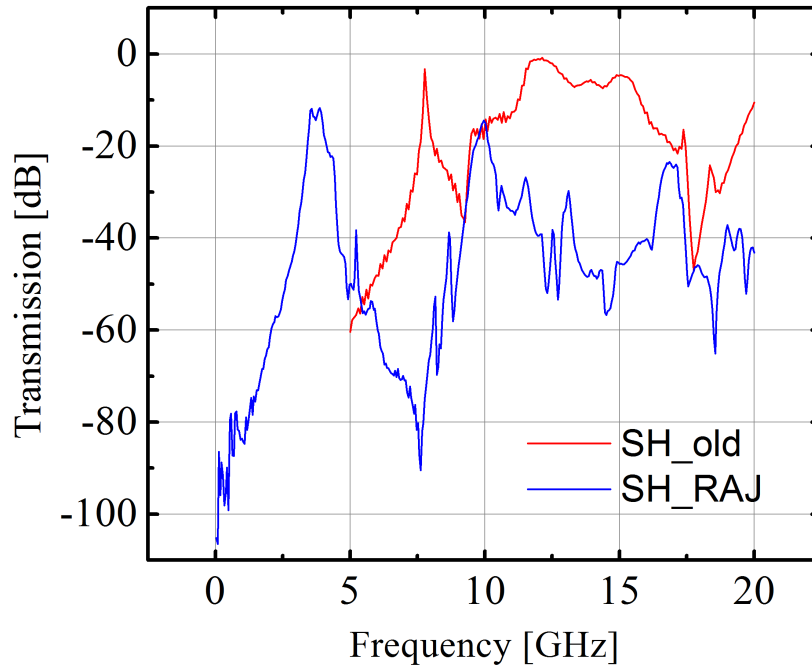


Figure F.33.: Old sample holder and new sample holder with PCB

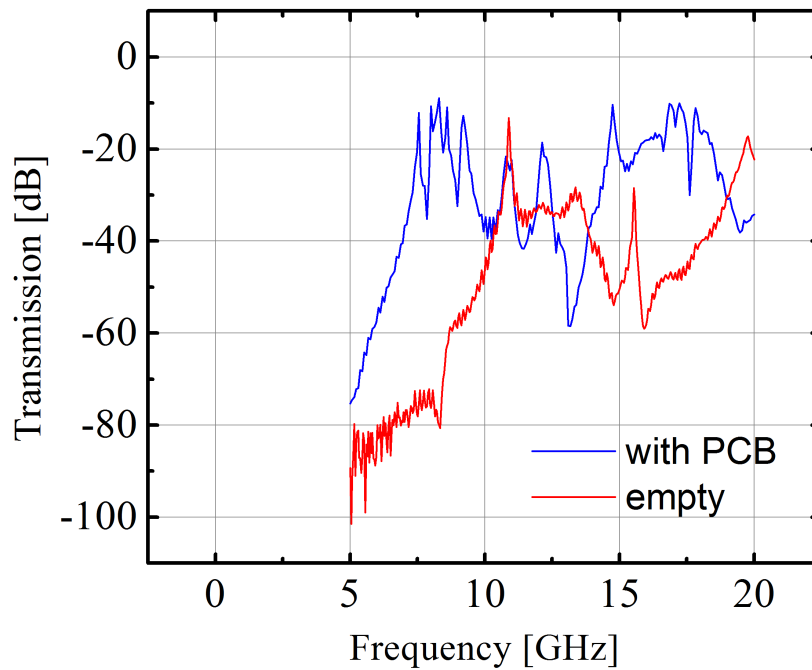


Figure F.34.: Bellshaped cavity with and without PCB

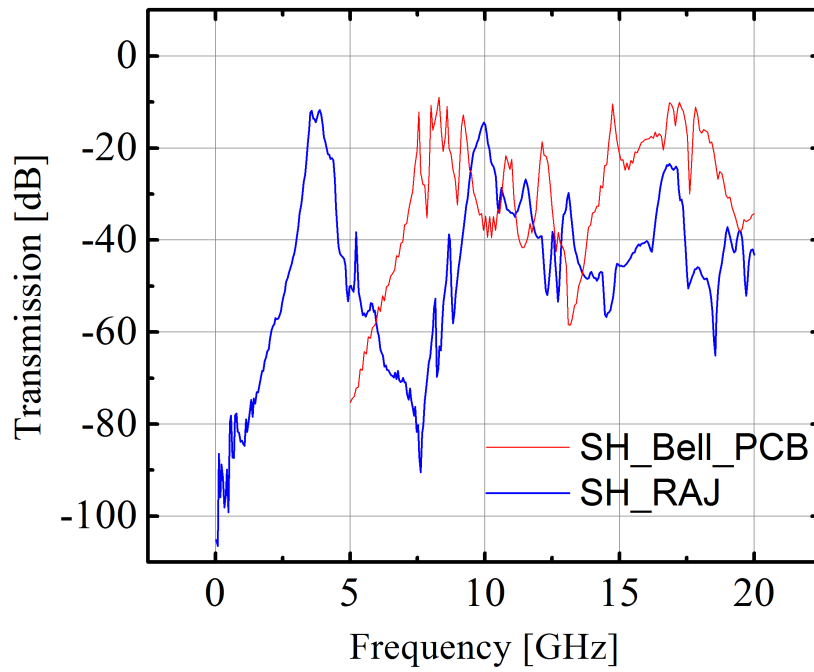


Figure F.35.: Bellshaped cavity and new sample holder with PCB

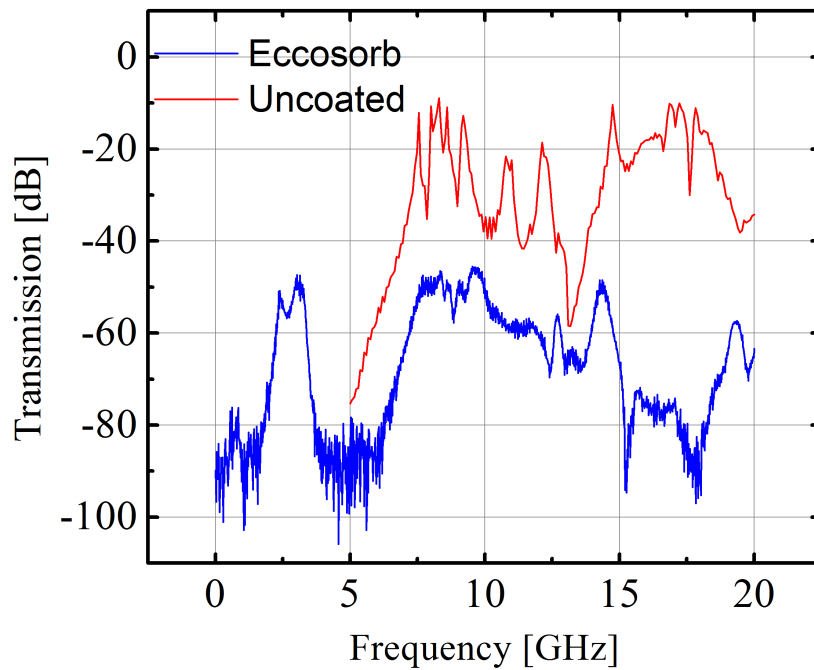


Figure F.36.: Bellshaped cavity with and without Eccosorb

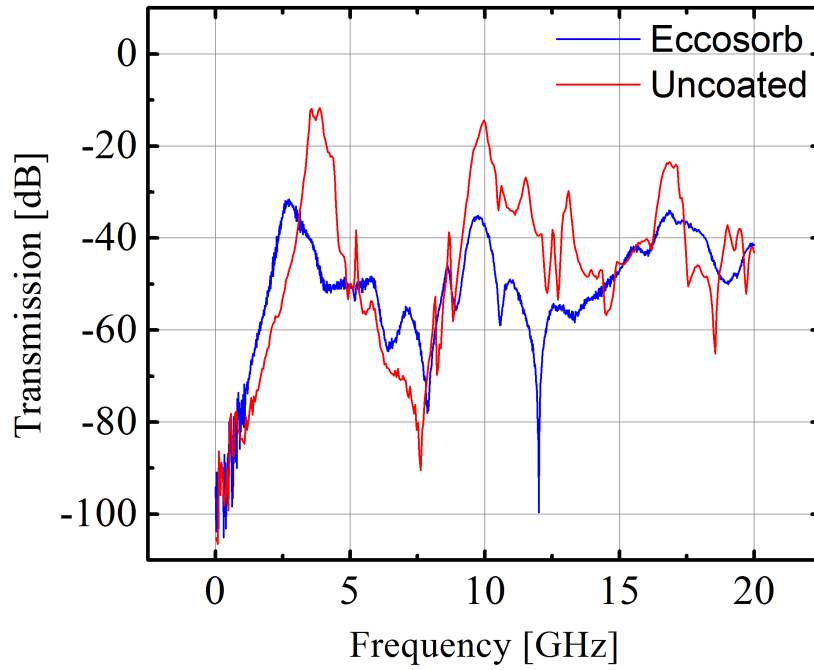


Figure F.37.: New sample holder with and without Eccosorb

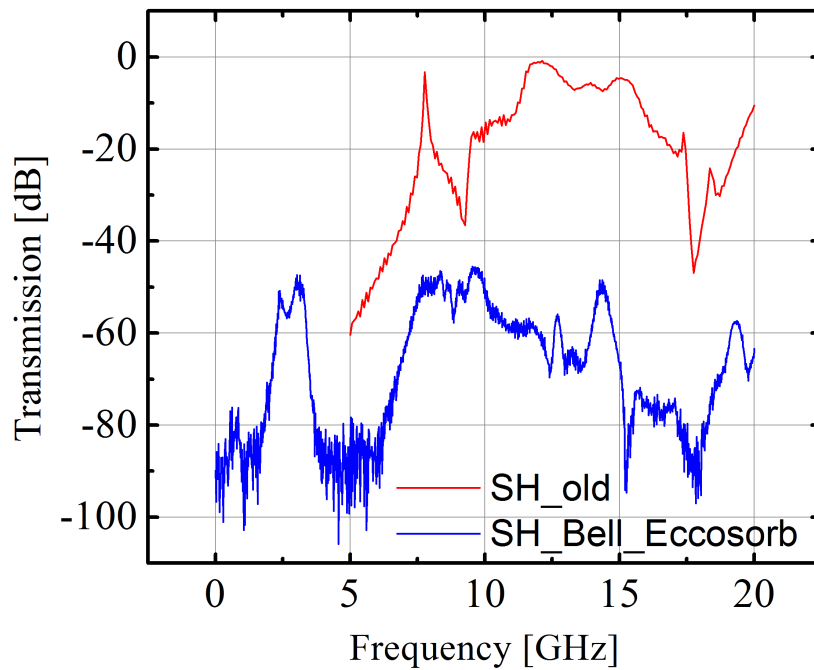


Figure F.38.: Old sample holder and bellshaped cavity with Eccosorb

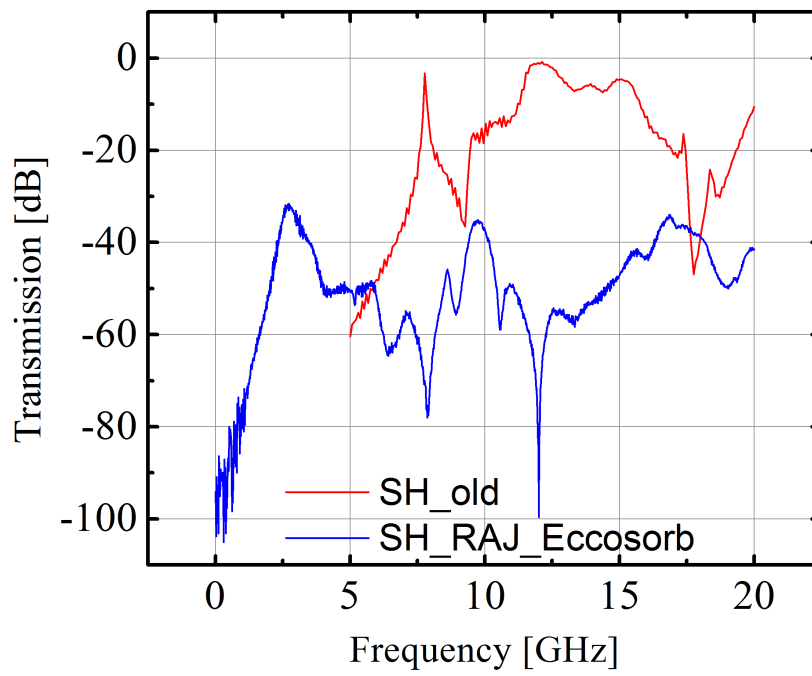


Figure F.39.: Old sample holder and new sample holder with Eccosorb